Received: 16 November 2017 | Revised: 12 July 2018 | Accepted: 13 July 2018

DOI: 10.1111/zsc.12309

ORIGINAL ARTICLE

WILEY Zoologica Scripta

An EPIC journey to locate single-copy nuclear markers in sea anemones

Mercer R. Brugler[1,2] | **Ricardo E. González-Muñoz**[3,4] | **Michael Tessler**[1] | **Estefanía Rodríguez**[1]

[1]Division of Invertebrate Zoology, American Museum of Natural History, New York, New York

[2]Biological Sciences Department, NYC College of Technology (CUNY), Brooklyn, New York

[3]Laboratorio de Biología de Cnidarios, Instituto de Investigaciones Marinas y Costeras (IIMyC), CONICET, Universidad Nacional de Mar del Plata, Mar del Plata, Argentina

[4]Instituto de Ciencias del Mar y Limnología (ICMyL), Posgrado en Ciencias del Mar y Limnología (PCMyL), UNAM, Ciudad Universitaria, Ciudad de México, México

Correspondence
Mercer R. Brugler, Biological Sciences Department, NYC College of Technology (CUNY), 300 Jay Street, Brooklyn, NY 11201.
Email: mbrugler@citytech.cuny.edu

Abstract

Sea anemones (Order Actiniaria) are among the most diverse members of the subclass Hexacorallia and are an emerging model system. Unfortunately, defining species and creating robust phylogenies remain a serious challenge due to simple body plans that reduce the number of available morphological characters, slow mitochondrial sequence evolution and a complete absence of nuclear markers in the actiniarian molecular toolkit other than the ribosomal cistron. Defining species boundaries and phylogenetic relationships is imperative for advancing our understanding of sea anemone taxonomy and systematics. Herein, we utilized EPIC (exon-priming intron-crossing) primers, in addition to non-standard PCR profiling conditions, to obtain sequence data for seven nuclear introns located within Calmodulin, Calpain, Nck Associated Protein 1 Homolog, Pescadillo Homolog, Signal Recognition Particle 54-kDa Subunit, Transferase and Vacuolar ATP Synthase Subunit B. These new markers were employed to evaluate whether morphological variability in marginal tentacle protuberances is indicative of intraspecific variation or cryptic species in the shallow-water anemone *Phymanthus crucifer*. Variability within these nuclear introns was compared to mitochondrial 12S, 16S and *cox3*, and nuclear 18S and 28S. PCR products of all nuclear introns were cloned to determine copy number and the resulting variability among clones was consistent with single-copy markers. We also amplified and sequenced six of the seven introns in a sister species, *Phymanthus loligo*, to determine the degree of interspecific variation. In addition, we evaluate the applicability of a subset of these markers within *Actinostola* and conclude with a review of putative single-copy markers used in octocoral and scleractinian phylogenetics.

KEYWORDS

Actiniaria, *Actinostola*, EPIC primers, Hexacorallia, *Phymanthus*, ribosomal cistron

1 | INTRODUCTION

Sea anemones sensu stricto (Order Actiniaria) are among the most diverse members of the subclass Hexacorallia and are an emerging model system, as they represent a basal eumetazoan lineage that serves as an outgroup to studies analysing the origin of one of the most significant shifts in animal evolution—the bilaterian body plan. However, simple body plans reduce the number of morphological characters available to define a species or provide phylogenetic information. Furthermore,

the limited number of morphological characters display extreme variability (e.g., the shape of muscles; arrangement of, and distribution of gametogenic tissue on, the mesenteries; structures on the column surface; arrangement and number of tentacles; cnidae, etc.) and homoplasy (e.g., presence of acontia, basilar muscles, etc.), making it difficult to establish natural divisions among species. Thus, mosaics of characters currently distinguish sea anemones. In fact, proposed evolutionary relationships have been largely based on an absence of features (see Carlgren, 1949), which is generally considered a fallacy in modern synapomorphy-based systematics.

Prior to a recent revision by Rodríguez et al. (2012), the traditional classification scheme within the Actiniaria, derived from Carlgren (1949), comprised of three suborders: Endocoelantheae, Nynantheae and Protantheae. A fourth suborder, Ptychodacteae, was later introduced by Cappola and Fautin (2000). Because each subordinal group was recognized by a unique feature (or the absence of a feature characterizing the other three), there was no clear relationship among the suborders. Early molecular phylogenetic reconstructions demonstrated the inadequacy of traditional morphological-based classifications for the Actiniaria (Daly, Chaudhuri, Gusmão, & Rodriguez, 2008; Daly, Fautin, & Cappola, 2003; Gusmão & Daly, 2010; Rodríguez, Barbeitos, Daly, Gusmao, & Häussermann, 2010; Rodríguez & Daly, 2008); all superfamilial groups and most families and genera were not monophyletic. However, when Rodríguez et al. (2012) recently revised the order Actiniaria based on a comprehensive molecular phylogeny that included representatives of all previously recognized suborders, the new higher level classification was composed of only two suborders, Anenthemonae and Enthemonae. Additionally, the authors found that the order Actiniaria was not even monophyletic; the deep sea anemone *Boloceroides daphneae* Daly, 2006, previously included within the infraorder Boloceroidaria, grouped sister to a clade containing members of the order Zoantharia (*B. daphneae* was reclassified as *Relicanthus daphneae* [Daly, 2006] within the family Relicanthidae, and *incerti ordinis* within the subclass Hexacorallia; Rodríguez et al., 2012). By removing *R. daphneae* from the Actiniaria, the order is once again considered monophyletic.

In addition to simple body plans and a limited number of morphological characters, sea anemones are members of the class Anthozoa, a group of animals characterized by exceptionally low rates of mitochondrial DNA sequence evolution (i.e., the synonymous substitution rate is 50–100 times slower than most metazoans; Hellberg, 2006). With few exceptions (i.e., cerianthids [Stampar, Maronna, Kitahara, Reimer, & Morandini, 2013] and select octocorals [McFadden et al., 2011], anemones [González-Muñoz et al., 2015] and scleractinians [Chen, Chiou, Dai, & Chen, 2008; Chen, Dai, Plathong, Chiou, & Chen, 2008; Chen et al., 2009]), variation within anthozoan mtDNA is almost non-existent at the intraspecific level (Brugler, Opresko, & France, 2013; Forsman, Barshis, Hunter, & Toonen, 2009; Hellberg, 2006; Shearer & Coffroth, 2002; Shearer, Van Oppen, Romano, & Wörheide, 2014; Thoma, Pante, Brugler, & France, 2007). In some instances, this lack of variability extends to commonly used nuclear genes; e.g., within black corals, nuclear ITS1 and ITS2 were unable to differentiate three morphologically disparate genera (Brugler et al., 2013), further emphasizing the need for more variable nuclear markers. Actiniarian systematists currently use a combination of five molecular markers (mitochondrial 12S [824 bp], 16S [428 bp] and *cox3* [636 bp] and nuclear 18S [~1,800 bp] and 28S [~3,300 bp]) to define species boundaries and infer phylogenetic relationships (e.g., Grajales & Rodríguez, 2016; Lauretta, Häussermann, Brugler, & Rodríguez, 2014). Unfortunately, *cox3* is not comparable across groups as *cox1* is the standard cytochrome c oxidase gene sequenced in other anthozoans. Daly, Gusmão, Reft, and Rodríguez (2010) compared phylogenetic signal in four of the five standard markers (*cox3* was not analysed) and recommended using 12S based on its effectiveness in recovering well-supported nodes (especially at lower levels) and amplicon length (one-third the size) when compared to 18S, the latter of which was found to be the second most effective gene at recovering relationships within Actiniaria. There are currently no widely used nuclear DNA markers in the actiniarian molecular toolkit other than the ribosomal cistron (18S-ITS1-5.8S-ITS2-28S; see usage of arginine kinase [*AK*] and a G-protein-coupled receptor [*GPCR*] by Geller, Fitzgerald, & King, 2005 and five stress-related genes [*ca2m*, *duf140*, *RNAbinding5*, *tyrK*, *sym32*] by Mallien et al., 2018). Daly et al. (2010) showed that 28S performed poorly when analysing a broad-scale dataset of sea anemones, displaying the most conflict among its primary trees (i.e., less resolution), was the least resolved individual dataset for a focused taxon sampling and had the lowest Data Decisiveness Index score when compared to 12S, 16S and 18S.

Nuclear markers remain elusive for sea anemones, black corals (Order Antipatharia), cerianthids (Subclass Ceriantharia) and zoantharians (Order Zoantharia). Locating variable, single-copy nuclear markers will allow actiniarian systematists to finally address fundamental questions, including: What is the biodiversity of sea anemones in a given environment or geographic region (i.e., how many species are present)?; What are the effects of dispersal and gene flow on population genetic structure, particularly in ephemeral environments (e.g., hydrothermal vent fields)?; What are the phylogenetic relationships among, and evolutionary history of, sea anemones?; and Which external and/or internal morphological characters are species specific? Defining species boundaries and deeper phylogenetic relationships is imperative and represents a critical

step in advancing our understanding of sea anemone taxonomy and systematics.

1.1 | *Phymanthus crucifer*: A case study

The actiniarian genus *Phymanthus* Milne-Edwards & Haime, 1851 currently contains 11 valid species (Daly & Fautin, 2018). *Phymanthus crucifer* (Le Sueur, 1817), commonly known as the beaded or speckled sea anemone, is a shallow-water actiniarian found in the Gulf of Mexico (hereafter abbreviated GoM), Caribbean and Bermuda (Gonzalez-Munoz, Simoes, Sanchez-Rodriguez, Rodriguez, & Segura-Puertas, 2012). There are three recognized morphotypes of *P. crucifer*: morphotype 1 contains lateral protuberances (papilliform or ramified) in the marginal tentacles; morphotype 2 lacks protuberances; and morphotype 3 is intermediate in form—some marginal tentacles have protuberances and others do not (protuberances will be referred to as ornamentation from this point forward) (see Figure 2 in González-Muñoz et al., 2015 for images of specimens examined). Verrill (1907, 2002) suggested that morphotypes 1 and 2 should be separate species, but also hypothesized that they could hybridize and create an intermediate form (i.e., morphotype 3). Duerden (1897, 1900, 1902) noted that the presence of intermediate forms suggests a continuum from with to without ornamentation and thus is indicative of a single species. A detailed morphological analysis of internal and external anatomy, as well as the cnidae, of *P. crucifer* by González-Muñoz et al. (2015) revealed no variation among the three morphotypes, lending support to the hypothesis of Duerden (i.e., a single species).

Herein, we utilize seven novel nuclear introns to evaluate whether morphological variability in marginal tentacle protuberances is indicative of intraspecific variation or cryptic species in the shallow-water sea anemone *P. crucifer*. Additionally, we discuss preliminary results regarding our evaluation of a subset of these nuclear markers in *Actinostola* Verrill, 1883, a genus characterized by species primarily from the deep sea and polar regions, and conclude with the putative single-copy nature of nuclear markers commonly used in octocoral and scleractinian phylogenetics.

2 | MATERIALS AND METHODS

2.1 | Sample collection

Eleven specimens (three of morphotype 1, three of morphotype 2 and five of morphotype 3) were collected from La Gallega Reef (19°13′13″N, 96°07′37″W) of the Veracruz Reef System in the GoM, two specimens (morphotypes 1 and 2) from Puerto Morelos Reef (20°55′50.7″N, 86°49′24″W) in the Mexican Caribbean (hereafter abbreviated MC) and one specimen (morphotype 3) from Punta Cancún (21°09′8.5″N, 86°44′22.5″W) in the MC, in 2010 (see Table 1 and Figure 1; assignment of numbers to the different morphotypes was arbitrarily conducted by RGM). Collections were conducted by hand, snorkelling or SCUBA

TABLE 1 List of *Phymanthus crucifer* specimens analysed in this study along with their respective morphotype designations and collection information

Specimen number	Morphotype designation	Collection locality	Latitude/Longitude	Depth (m)
RG-130	1	La Gallega Reef, Veracruz Reef System, Gulf of Mexico	19°13′17.22″/96°7′38.20″	<2
RG-133	1	La Gallega Reef, Veracruz Reef System, Gulf of Mexico	19°13′17.22″/96°7′38.20″	<2
RG-187B	1	La Gallega Reef, Veracruz Reef System, Gulf of Mexico	19°13′17.22″/96°7′38.20″	1–2
RG-219A	1	Puerto Morelos Reef, Quintana Roo, Mexican Caribbean	20°51′51.90″/86°51′28.10″	8
RG-131	2	La Gallega Reef, Veracruz Reef System, Gulf of Mexico	19°13′17.22″/96°7′38.20″	<2
RG-143	2	La Gallega Reef, Veracruz Reef System, Gulf of Mexico	19°13′17.22″/96°7′38.20″	<1
RG-182A	2	La Gallega Reef, Veracruz Reef System, Gulf of Mexico	19°13′17.22″/96°7′38.20″	1–2
RG-220A	2	Puerto Morelos Reef, Quintana Roo, Mexican Caribbean	20°55′50.7″/86°49′24.00″	10
RG-128	3	La Gallega Reef, Veracruz Reef System, Gulf of Mexico	19°13′17.22″/96°7′38.20″	<2
RG-129	3	La Gallega Reef, Veracruz Reef System, Gulf of Mexico	19°13′17.22″/96°7′38.20″	<2
RG-134	3	La Gallega Reef, Veracruz Reef System, Gulf of Mexico	19°13′17.22″/96°7′38.20″	<2
RG-138A	3	La Gallega Reef, Veracruz Reef System, Gulf of Mexico	19°13′17.22″/96°7′38.20″	<2
RG-184	3	La Gallega Reef, Veracruz Reef System, Gulf of Mexico	19°13′17.22″/96°7′38.20″	1–2
RG-200A	3	Punta Cancun, Quintana Roo, Mexican Caribbean	21°09′8.5″/86°44′22.5″	8
PHY	Not applicable	Acquired from a pet shop in Columbus, Ohio	N/A	N/A

Note. PHY: *Phymanthus loligo*. N/A: information not available.

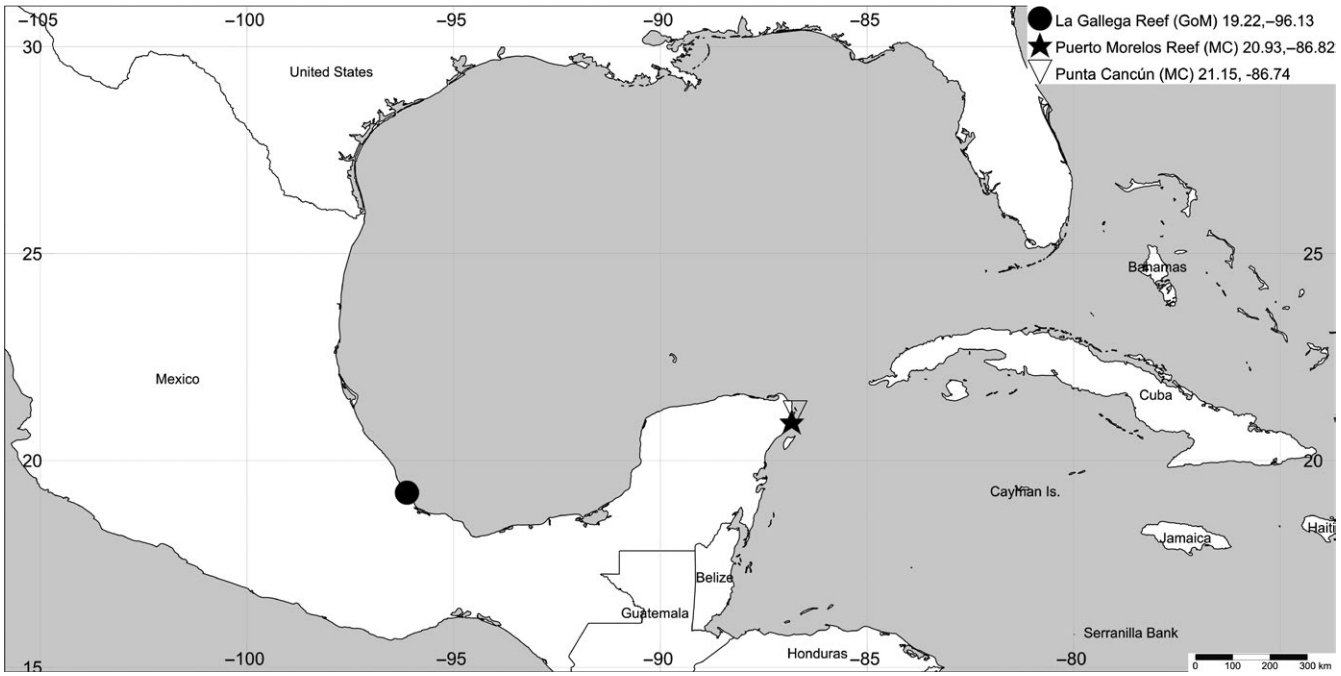

FIGURE 1 Sampling localities for specimens collected from La Gallega Reef ($n = 11$; circle), Puerto Morelos Reef ($n = 2$; star), and Punta Cancún ($n = 1$; inverted triangle). GoM: Gulf of Mexico; MC: Mexican Caribbean

diving, and utilized a hammer and chisel. Collected specimens were transferred to the laboratory and maintained in an aquarium allowing photographic documentation of their colour when alive. Subsamples of tissue were obtained from the pedal disc of all specimens and preserved in 96% ethanol. Whole specimens were then relaxed in 5% $MgSO_4$ seawater solution and fixed in 10% seawater-buffered formalin. All specimens were identified using polyp anatomy and the distribution and size of cnidae in various regions of the polyp. Voucher specimens were deposited in the Collection of Cnidarians of the GoM and MC Sea (Registration code: YUC–CC–254–11) of the Unidad Multidisciplinaria de Docencia e Investigación en Sisal (UMDI-Sisal) at the Universidad Nacional Autónoma de México (UNAM) and at the American Museum of Natural History (AMNH; accession number 65822).

2.2 | Development of primers for new nuclear markers

We surveyed the literature for anthozoan-specific EPIC (exon-priming intron-crossing) primer sets that claimed to amplify single-copy nuclear markers. We specifically targeted nuclear introns as they are putatively under less selective pressure than their surrounding exons and are therefore free to accumulate mutations. Using this method, we obtained primer sets for Calmodulin (*CaM*; Yuasa, Suzuki, & Yazawa,), Calpain (*i2*) and Transferase (*i50*; Chenuil et al., 2010), Vacuolar ATP Synthase Subunit B (*VATPS-β*; Bourlat, Nielsen, Economou, & Telford, 2008) and Signal Recognition Particle 54-kDa Subunit (*SRP54*; Jarman, Ward, & Elliott, 2002). All published primers were compared to existing sea anemone sequence data (e.g., the *Nematostella vectensis* Stephenson, 1935 nuclear genome; assembly ASM20922v1) to make sea anemone-specific primers; the only exception was Transferase (*i50*), for which sea anemone sequence data was not available. We also developed new EPIC primers based on sequences obtained from UniProt (Universal Protein Resource; The UniProt Consortium 1900). These primers, designed to amplify Nck Associated Protein 1 Homolog (*Nck*) and Pescadillo Homolog (*Pes*), were also compared to existing sea anemone sequence data to make sea anemone-specific primers. In some cases, following initial amplification and sequencing, internal primers were developed using *Phymanthus*-specific DNA sequence data (i.e., for *i2*, *Nck* and *Pes*).

2.3 | Molecular data acquisition

DNA extraction, DNA quantification, PCR reagents, PCR cleanup, cycle sequencing, cycle sequencing cleanup and Sanger sequencing on an ABI-3730xL followed the protocols detailed in Lauretta et al. (2014). Table 2 contains the primers used to amplify the five standard genes used in actiniarian phylogenetics (i.e., mitochondrial 12S, 16S and *cox3* and nuclear 18S and 28S) while Table 3 contains optimized PCR thermocycling profiles for each primer set. Table 4 contains the primers used to amplify the seven new nuclear DNA markers while Table 5 contains optimized PCR thermocycling profiles for each primer set. To obtain initial PCR amplification of the new nuclear markers, we utilized

TABLE 2 List of primers used to amplify the five standard genes utilized in actiniarian phylogenetics, including their melting temperature (T_M; per Integrated DNA Technologies), length, number of ambiguities and sequence. See Table 3 for recommended primer combinations and thermocycling profiles

Primer name	T_M (°C)	Length (bp)	Number of ambiguities	Sequence (5′–3′)
12S-Forward	57.9	24	0	AGC CAC ACT TTC ACT GAA ACA AGG
12S-Reverse	59.3	27	6	GTT CCC YYW CYC TYA CYA TGT TAC GAC
16S-Forward	56.8	23	0	CAC TGA CCG TGA TAA TGT AGC GT
16S-Reverse	53.5	21	0	CCC CAT GGT AGC TTT TAT TCG
CO3-Forward	57.2	26	0	CAT TTA GTT GAT CCT AGG CCT TGA CC
CO3-Reverse	55.2	28	0	CAA ACC ACA TCT ACA AAA TGC CAA TAT C
18S-A	58.9	21	0	AAC CTG GTT GAT CCT GCC AGT
18S-L	51.8	22	0	CCA ACT ACG AGC TTT TTA ACT G
18S-C	53.0	21	0	CGG TAA TTC CAG CTC CAA TAG
18S-Y	56.5	21	0	CAG ACA AAT CGC TCC ACC AAC
18S-O	60.9	21	0	AAG GGA CCA CCA GGA GTG GAG
18S-B	60.6	22	0	TGA TCC TTC CGC AGG TTC ACC T
5S	61.6	25	0	GCC GAC CCG CTG AAT TCA AGC ATA T
R635	56.2	19	0	GGT CCG TGT TTC AAG ACG G
F635	56.2	19	0	CCG TCT TGA AAC ACG GAC C
R1630	57.3	20	5	CCY TTC YCC WCT CRG YCT TC
F1379	63.6	22	1	GAC AGC AGG ACG GTG GYC ATG G
R2077	58.2	23	2	GAG CCA ATC CTT WTC CCG ARG TT
F2076	57.7	24	2	TAA CYT CGG GAW AAG GAT TGG CTC
R2800	59.8	22	2	GAG CTY RCC TTA GGA CAC CTG C
F2800	59.8	22	2	GCA GGT GTC CTA AGG YRA GCT C
R3264	55.4	21	1	TTC YGA CTT AGA GGC GTT CAG

non-standard PCR profiling conditions with respect to annealing (≥45°C for 1 min) and extension (68°C for 1 min and 30 s) temperatures, followed by a gradient of increasing annealing temperatures to eliminate non-specific amplification (i.e., sub-banding).

2.4 | Cloning

All seven nuclear genes were newly amplified immediately prior to cloning. To ligate PCR products into the vector, the following TA Cloning® Kit reagents (Invitrogen) were

TABLE 3 PCR thermocycling profiles used to amplify the five standard genes utilized in actiniarian phylogenetics. Mitochondrial genes received an initial denature temperature of 94°C for 2 min. Nuclear 18S and 28S received an initial denature temperature of 94°C for 5 min. 18S is amplified in three reactions and 28S is amplified in five reactions. Mt: mitochondrial

Primer combination	Approximate length (bp)	Denature	Annealing	Extension	Repeat	Final extension
Mt 12S	824	94°C/20 s	55.0°C/30 s	72°C/50 s	40	72°C/5 min
Mt 16S	428	94°C/20 s	51.5°C/30 s	72°C/45 s	35	72°C/4 min
Mt *cox3*	636	94°C/20 s	51.0°C/30 s	72°C/45 s	40	72°C/5 min
Nuclear 18S: A-L	639	94°C/30 s	52.0°C/45 s	72°C/45 s	40	72°C/6 min
Nuclear 18S: C-Y	732	94°C/30 s	53.0°C/45 s	72°C/45 s	40	72°C/6 min
Nuclear 18S: O-B	645	94°C/30 s	58.0°C/45 s	72°C/45 s	40	72°C/6 min
Nuclear 28S: 5S-R635	800	94°C/30 s	56.0°C/45 s	72°C/45 s	40	72°C/6 min
Nuclear 28S: F635-R1630	850	94°C/30 s	56.0°C/45 s	72°C/45 s	40	72°C/6 min
Nuclear 28S: F1379-R2077	742	94°C/30 s	60.0°C/45 s	72°C/45 s	40	72°C/6 min
Nuclear 28S: F2076-R2800	751	94°C/30 s	58.0°C/45 s	72°C/45 s	40	72°C/6 min
Nuclear 28S: F2800-R3264	465	94°C/30 s	55.0°C/45 s	72°C/40 s	40	72°C/6 min

combined in 0.2 ml PCR tubes: 0.8 µl dH_2O, 0.2 µl 10X Ligation Buffer, 0.2 µl T4 DNA Ligase (4.0 Weiss units) and 0.4 µl pCR®2.1 vector (25 ng/µl) for a total volume of 1.6 µl. We then added 0.4 µl of fresh PCR product to each 0.2 ml PCR tube and incubated the ligation reaction at +4°C for 48 hr. To prepare agar plates, two packets of imMedia™ Amp Blue growth medium (for lacZ+ Amp recombinant *E. coli* strains; Invitrogen) were combined with 400 ml dH_2O in a sterile glass flask. The mixture was heated in a microwave and poured into sterile petri dishes (lids removed to prevent condensation). Two plates were prepared for each PCR product to allow plating of 50 µl (onto plate 1) and 100 µl (onto plate 2) of a single transformed product (plates containing 100 µl of transformed product can become overcrowded with colonies, making individual colony selection difficult; thus, also preparing a 50 µl transformation is advised). A single 50 µl tube of One Shot® TOP10 Chemically Competent *E. coli* cells (Invitrogen) was used to process two ligated PCR products (25 µl each). The 50 µl tubes of *E. coli* cells were thawed for 30 min on ice, after which 25 µl of *E. coli* cells were distributed into new prechilled 1.5-ml microcentrifuge tubes. The ligation reaction mix (2 µl) was then added to the 25 µl of *E. coli* cells (total: 27 µl), stirred with a pipette tip and incubated for 30 min on ice. The *E. coli* cells were heat shocked in a 42°C water bath for 30 s and immediately placed on ice for 2 min. S.O.C. medium was warmed by hand prior to adding 125 µl to each tube. The tubes were placed horizontally in an incubator at 37°C and shaken at 225 RPM for 3 hr. Agar plates that were not prepared fresh were warmed to 37°C prior to plating. For each tube, 100 µl of transformation was pipetted onto one plate and 50 µl onto a second plate. A sterile glass rod spreader (Carolina Biological Supply) was used to spread the mixture around the plate in a circular pattern, followed by incubation at room temperature for 5–10 min. The plates were flipped upside-down (agar on top) and incubated at 37°C overnight. Following overnight incubation, plates were transferred to +4°C for 2–3 hr to allow for proper colour development of the blue colonies. We sampled upwards of 14 white colonies per PCR product using pipette tips and subsequently placed those pipette tips into 0.2 µl-PCR tubes containing the same 25-µl PCR mastermix detailed in Lauretta et al. (2014) (an extra 1 µl of dH_2O was added to replace the 1 µl of template not being added). The only exception was the use of M13 primers (10 µM concentration; M13 forward: 5′-GTA AAA CGA CGG CCA GT-3′; M13 reverse: 5′-CAG GAA ACA GCT ATG AC-3′). The pipette tip was kept in the PCR tube until all tubes had been processed. Prior to removing the pipette tip from the PCR tube, we pipetted up and down, and stirred, to mix the *E. coli* into the mastermix. The PCR tubes were placed in a thermocycler and the inserts were amplified using the M13 profile, as follows: initial denature at 95°C for 3 min; denature at 95°C for 20 s; anneal at 50°C for 20 s; extend at 72°C for 2 min; repeat steps 2–4 for 35 cycles; final extension at 72°C for 10 min. PCR cleanup, cycle sequencing, cycle sequencing cleanup and Sanger sequencing followed the protocols detailed in Lauretta et al. (2014).

2.5 | Phylogenetic reconstruction of concatenated mitochondrial DNA

All sequence traces were edited using Sequencher™ v5.0.1 (Gene Codes Corp.) and subsequently transferred to Se-Al v2.0a11 Carbon. Gene identity was verified with BLAST

TABLE 4 List of primers used to amplify the seven novel nuclear DNA markers, including their melting temperature (T_M; per Integrated DNA Technologies), length, number of ambiguities, and sequence. F: forward primer. R: reverse primer. E: exon. ACT: actiniarian-specific primer. NV: *Nematostella vectensis*-specific primer. Phy: *Phymanthus*-specific primer. LA: long allele (details regarding the short allele are not included)

Gene	Primer name	T_M (°C)	Length (bp)	Number of ambiguities	Sequence (5′–3′)
Calmodulin[a]	CaM-E3-F	53.0	20	1	GAC GGC AAT GGY TTT ATC AG
	CaM-E4-R	51.1	24	1	CTT TGA TGT CAT CAT YTT CAC AAA
Calpain[b]	i2-NV-F	63.7	32	0	TAC ATG AAG GTG ATG GGT GGG TAC GAC TTT CC
	i2-Phy-R	57.9	22	0	GCC AGT AAG AGC ATG AAG GTC G
Vacuolar ATP Synthase Subunit B[c]	VATPS-ACT-F	55.6	22	2	GGM TCW ATG GAA AAT GTG TGC C
	VATPS-ACT-R	62.1	20	2	GGG AAA CCA CGR CGW CCA GG
Signal Recog. Part. 54-kDa Subunit[d]	SRP54-NV-F	62.0	35	0	ATG GGG GAT ATT GAA GGT CTG ATT GAC AAA GTC AA
	SRP54-NV-R	57.3	32	2	TTC ATG ATR TTY TGG AAC TGT TCA TAC ATG TC
Pescadillo Homolog[e]	Pes-Phy-F	59.6	25	0	CAG GTA TAG CAG CCG CAA GTA TTG G
	Pes-Phy-R	56.8	26	0	CTG TGG TTT GTC TTA GCT CTC ATA GG
Nck Associated Protein 1 Homolog[f]	Nck-Phy-LA-F	59.8	23	0	GCC ACG GAA GAG AAA AGG AGG AC
	Nck-Phy-LA-R	64.2	20	0	GCC CAG GAA TGG TGG CTG CC
Transferase[g]	i50-F	60.6	32	2	GAT GGA ATC CAT GTC TTG GTC AAY ATG AAY GG
	i50-R	63.4	32	2	GTG ACC GAG TCG GTG ATC AGG TAR TCC ATR AA

[a]Forward primer sits within exon 3 of the *Metridium senile CaM* gene [see figure 3 in Yuasa et al. ()]; used sequences of *M. senile* and *N. vectensis* to develop primer. Reverse primer sits within exon 4 of the *M. senile CaM* gene; used sequences of *M. senile, N. vectensis,* and *Acropora muricata* to develop primer—relied primarily on comparison to *N. vectensis* and *A. muricata*.[b]Compared Chenuil et al. (2010) forward primer to *N. vectensis* to make anemone-specific primer for Calpain. We were unable to align the reverse primer to *N. vectensis,* so after obtaining preliminary sequence, we made an internal, *Phymanthus crucifer*-specific, reverse primer for Calpain.[c]Forward primer listed in Bourlat et al. (2008) spans an intron in *N. vectensis* so had to develop a different primer; primer developed using *Uticina eques* and *N. vectensis;* primer is 28 bp upstream from the end of exon 9. Reverse primer listed in Bourlat et al. (2008) also spans an intron in *N. vectensis* so had to develop a different primer; primer developed using *U. eques* and *N. vectensis;* primer is 26 bp downstream from the beginning of exon 11; primers cross two introns (115 bp and 199 bp) that are separated by exon 10 (122 bp).[d]Compared Jarman et al. (2002) forward primer to *N. vectensis* to develop primer; appears that *SRP54* not sequenced for *Aiptasia pallida* or *A. pulchella;* primer sits 51 bp upstream of the end of the exon. Compared Jarman et al. (2002) reverse primer to *N. vectensis* to develop primer; primer sits 16 bp downstream from the beginning of the exon; primers span a 100 bp intron.[e]Initially compared *N. vectensis Pes* sequence to *Hydra magnipapillata Pes* gene to make *Pes* primers. After obtaining preliminary sequence, we made internal, *P. crucifer*-specific, *Pes* primers.[f]Initially compared *N. vectensis Nck* sequence to the *Nck* genes of *Branchiostoma floridae* (lancelet), *Xenopus tropicalis* (frog) and *Loxodonta africana* (elephant) to make *Nck* primers. After obtaining preliminary sequence, we made internal, *P. crucifer*-specific, *Nck* primers.[g]We could not align Chenuil et al. (2010) forward and reverse primers to any available anemone sequence data so both primers are exactly as presented in Chenuil et al. (2010).

(Altschul, Gish, Miller, Myers, & Lipman, 1990). Herein we provide new sequences for *Phymanthus crucifer*, which we added to the dataset presented in Rodríguez et al. (2012). With the exception of the black coral *Leiopathes glaberrima* (Esper, 1788), all outgroups were removed from the dataset. Due to the inability to obtain *Phymanthus*-specific 18S and

28S sequence using the standard primers, we did not include any nuclear sequence in the final dataset. Thus, the concatenated dataset, consisting of mitochondrial 12S, 16S and *cox3*, contained 115 taxa and 2,697 sites. For complete details of taxa included in this study, we refer readers to Rodríguez et al. (2012). New sequences have been deposited in GenBank (Table 6).

Prior to concatenating all three mitochondrial genes, each gene region was separately aligned with MAFFT v7 (http://mafft.cbrc.jp/alignment/server/) using the following parameters: strategy = L-INS-I; scoring matrix = 200PAM/k = 2; gap open = 1.53; gap offset = 0.05 (Katoh, Misawa, Kuma, & Miyata, 2002; Katoh, Kuma, Toh, & Miyata, 2005; alignment available upon request). Akaike information criterion (AIC) was implemented within jModelTest v2.1.2 (Darriba, Taboada, Doallo, & Posada, 2012) to determine the appropriate evolutionary model (TIM2 + I+G) and corresponding parameters [p-inv = 0.0470; gamma shape = 0.3360; freqA = 0.3034; freqC = 0.1821; freqG = 0.2212; freqT = 0.2933; (AC) = 1.3194; (AG) = 5.0386; (AT) = 1.3194; (CG) = 1.0000; (CT) = 8.7441; (GT) = 1.0000] for the concatenated dataset (number of candidate models: 88; number of substitution schemes: 11; base tree for likelihood calculations: BIONJ using PhyML v3.0 [Guindon et al., 2010]). We searched for optimal trees using maximum likelihood (ML) within PhyML v3.0 (http://www.atgc-montpellier.fr/phyml/; Guindon & Gascuel, 2003). The following parameters were implemented within PhyML: substitution model = GTR+I+G (the online version of PhyML does not implement TIM2, and GTR had a ΔAIC of 2.3); substitution rate categories = 6; p-inv and gamma shape = per jModelTest; starting tree = BIONJ; tree improvement = SPR and NNI; optimized tree topology and branch lengths; bootstrap replicates = 350.

2.6 | Obtaining *Phymanthus*-specific 18S and 28S sequence data

To obtain *Phymanthus*-specific rDNA, we implemented two protocols. For 18S, we aligned the 18S gene of *Symbiodinium* Freudenthal, 1962 with all available sea anemone 18S sequences and designed new primers in regions that contained ambiguities in the *Symbiodinium* sequence but not in the sea anemone sequence (primer sequences are available in Grajales & Rodríguez, 2016). For 28S, we paired antipatharian-specific 28S primers (see Brugler et al., 2013) with the standard sea anemone 28S primers (Table 7). The only antipatharian-specific 28S primers that were not published in Brugler et al. (2013) are 28Santi1163F (5′-GAG GTC TTA GGG TTA AAA CAA CC-3′) and 28Santi2100R (5′-CTT CAA GTC YCA GCC CGA CAG-3′). All resulting *Phymanthus*-specific 18S and 28S sequences were separately added to the dataset presented in Rodríguez et al. (2012), thus creating two datasets. With the exception of the black coral *L. glaberrima*, all outgroups were removed. The 18S dataset contained 118 taxa and 2,176 sites and the 28S dataset contained 118 taxa and 4,082 sites. New sequences have been deposited in GenBank (Table 6). Multiple sequence alignment used MAFFT v7 as above (alignment available upon request). AIC was implemented within jModelTest v2.1.2 (as above) to determine the appropriate evolutionary model and corresponding parameters for 18S (model = TIM2 + I+G; p-inv = 0.3990; gamma shape = 0.3730; freqA = 0.2149; freqC = 0.2670; freqG = 0.3115; freqT = 0.2066; [AC] = 0.6582; [AG] = 2.2170; [AT] = 0.6582; [CG] = 1.0000; [CT] = 4.7568; [GT] = 1.0000) and 28S (model = GTR+I+G; p-inv = 0.4180; gamma shape = 0.4140; freqA = 0.2071; freqC = 0.2807; freqG = 0.3153; freqT = 0.1969; [AC] = 0.5542;

TABLE 5 Optimized PCR thermocycling profiles used to amplify the seven novel nuclear DNA markers in *Phymanthus crucifer* and *P. loligo*. An initial denature temperature of 94°C for 3 min was utilized in all cases. Note the non-standard extension temperature of 68°C in some profiles

Gene region	Length (bp)	Denature	Annealing	Extension	Repeat	Final extension
Calmodulin *(CaM)*	447, 449	94°C/1 min	45.0°C/1 min	68°C/1 min & 30 s	45	68°C/6 min
Calpain (*i2*)	128	94°C/1 min	53.0°C/1 min	68°C/1 min & 30 s	45	68°C/6 min
Vacuolar ATP Synthase Subunit B *(VATPS-β)*	584, 585	94°C/1 min	48.6°C/1 min	72°C/1 min & 30 s	45	72°C/6 min
Signal Recog. Particle 54-kDa Subunit (*SRP54*)[a]	509, 515	94°C/1 min	45.0°C/1 min	68°C/1 min & 30 s	45	68°C/6 min
Pescadillo Homolog (*Pes*)	234	94°C/1 min	48.0°C/1 min	72°C/1 min & 30 s	45	72°C/6 min
Nck Associated Protein 1 Homolog (*Nck*)	509	94°C/1 min	45.2°C/55 s	72°C/40 s	40	72°C/6 min
Transferase (*i50*)	789	94°C/1 min	45.0°C/1 min	72°C/1 min & 30 s	45	72°C/6 min

[a]Amplicon lengths include both RG-187B (509 bp) and RG-219A (509 and 515 bp).

TABLE 6 GenBank accession numbers for the five standard genes and seven new nuclear DNA markers for all *Phymanthus crucifer* specimens analysed in this study. GenBank accession numbers are also provided for *P. loligo* (specimen #PHY)

Specimen Number	Morphotype Designation	Standard Genes				
		12S	16S	*cox3*	18S	28S
RG-130	1	Identical[a]	Identical[a]	Identical[a]	MH670399	MH670928
RG-133	1	Identical[a]	Identical[a]	Identical[a]	MH670400	MH670930
RG-187B	1	Identical[a]	Identical[a]	Identical[a]	MH670401	MH670935
RG-219A	1	Identical[b]	Identical[a]	Identical[a]	N/A	MH670936
RG-131	2	Identical[a]	Identical[a]	Identical[a]	MH670403	MH670929
RG-143	2	Identical[b]	Identical[a]	Identical[a]	MH670405	MH670933
RG-182A	2	KJ910343	KJ910345	KJ910346	N/A	N/A
RG-128	3	Identical[a]	Identical[a]	Identical[a]	MH670397	MH670926
RG-129	3	Identical[b]	Identical[a]	Identical[a]	MH670398	MH670927
RG-134	3	Identical[b]	Identical[a]	Identical[a]	MH670402	MH670931
RG-138A	3	KJ910344	Identical[a]	Identical[a]	N/A	MH670932
RG-184	3	Identical[a]	Identical[a]	Identical[a]	MH670404	MH670934
PHY	N/A	EU190745	EU190791	GU473345	EU190871	N/A

Specimen Number	Morphotype Designation	Novel Nuclear DNA Markers						
		CaM	*i2*	*VATPSb*	*SRP54*	*Pes*	*Nck*	*i50*
RG-015	N/A	N/A	N/A	N/A	N/A	MH682111	N/A	N/A
RG-030	N/A	N/A	N/A	N/A	N/A	MH682112	N/A	N/A
RG-187B	1	MH682131	MH682104	MH682136	MH682128	MH682115	MH682122	MH682108
RG-219A	1	MH682133	MH682101	MH682137	MH682129	MH682117	MH682124	MH682109
RG-182A	2	N/A	MH682103	N/A	N/A	MH682114	MH682121	N/A
RG-220A	2	N/A	MH682106	N/A	N/A	MH682118	MH682125	N/A
RG-138A	3	MH682132	MH682100	MH682135	MH682127	MH682113	MH682120	MH682107
RG-200A	3	N/A	MH682105	N/A	N/A	MH682116	MH682123	N/A
PHY	N/A	MH682130	MH682102	MH682134	MH682126	MH682110	MH682119	N/A

[a]Shares an identical haplotype with specimen # RG-182A. [b]Shares an identical haplotype with specimen # RG-138A. N/A: Sequence data or information not available.

TABLE 7 PCR primer combinations and thermocycling profiles used to amplify anemone-specific 28S in *Phymanthus crucifer*. All reactions received an initial denature temperature of 94°C for 5 min and a final extension temperature of 72°C for 6 min

Primer combination	Approximate length (bp)	Denature	Annealing	Extension	Repeat
28Santi123F-R635	660	94°C/30 s	56.0°C/45 s	72°C/40 s	45
28Santi123F-28Santi1078R	1,020	94°C/30 s	56.0°C/45 s	72°C/55 s	45
28Santi1163F-R1630	460	94°C/30 s	49.0°C/45 s	72°C/30 s	45
F1379-28Santi2100R	760	94°C/30 s	54.0°C/45 s	72°C/40 s	40
28Santi1911F-R2800	940	94°C/30 s	60.0°C/45 s	72°C/50 s	45
28Santi2693F-28Santi3461R	930	94°C/30 s	58.0°C/45 s	72°C/45 s	45

[AG] = 2.0211; [AT] = 0.8583; [CG] = 0.9551; [CT] = 5.2254; [GT] = 1.0000). We searched for optimal trees using PhyML v3.0. The following parameters were implemented within PhyML for both 18S and 28S: substitution model = GTR+I+G (for 18S, GTR+I+G had a ΔAIC of 0.6866); substitution rate categories = 6; p-inv and gamma shape = per jModelTest; starting tree = BIONJ; tree improvement = SPR and NNI; optimized tree topology and branch lengths; bootstrap replicates = 350.

3 | RESULTS

3.1 | Variation in mitochondrial DNA among *Phymanthus crucifer* morphotypes

As first reported by González-Muñoz et al. (2015), comparison of aligned sequences for *cox3* (663 bp) and 16S (428 bp) did not reveal any variation among individuals or morphotypes of *Phymanthus crucifer* from the GoM or MC. However, mitochondrial 12S (824 bp) revealed two haplotypes that were distinguished by a single substitution (K2P distance = 0.1215%), but these haplotypes were not specific to any particular morphotype. While haplotype 1 (H1; differentiated by a single adenine substitution) was specific to GoM specimens, it was shared by all three morphotypes. Haplotype 2 (H2; differentiated by a single guanine substitution) was more broadly distributed, being shared between specimens in the GoM and MC. Within the GoM, H2 was shared by morphotypes 2 and 3, while in the MC it was shared by all three morphotypes. *Phymanthus loligo* (Hemprich and Ehrenberg in Ehrenberg, 1834) shares an identical 12S sequence (across 812 bp) with *P. crucifer* H2, but has a K2P distance of 0.1233% when compared to *P. crucifer* H1. The mtDNA-based phylogenetic reconstruction recovered the two 12S-based *P. crucifer* haplotypes as sister taxa, and these as sister to *P. loligo* (Figure 2). However, *Heteranthus* sp. was recovered as sister to the actiniid genus *Anemonia* Risso, 1826, rending the Phymanthidae polyphyletic.

3.2 | Variation in nuclear rDNA among *Phymanthus crucifer* morphotypes

Using newly designed 18S primers, we obtained nearly complete 18S sequence data for eight individuals from the GoM (representing all three morphotypes; see Table 6 for GenBank accession numbers). We were unable to obtain 18S data for specimens from the MC. We uncovered intra-individual variation in specimen RG-184 (morphotype 3) from the GoM. Three different primer sets (18SNO-18SNBmod, 18SNC-18SNBmod, 18SNC-18SNY) were used to amplify 1,143 bp of 18S in this specimen, revealing eight variable sites across 662 comparable bases (K2P distance = 1.22%; the contig is comprised of three [original] partially overlapping amplicons, not cloned PCR products). Intra-individual variation has been found in 28S sequences of some octocorals and antipatharians (MRB, personal observation), but this is the first example of intra-individual variation in 18S within anthozoans. All *Phymanthus* 18S sequences were added to the comprehensive dataset presented in Rodríguez et al. (2012) and a phylogeny was constructed using maximum likelihood (Figure 3). The eight individuals of *P. crucifer* formed a monophyletic clade that grouped sister to *Bunodactis verrucosa* (Pennant, 1777) (Actiniidae; bootstrap support: 57%). 18S data revealed that *P. loligo* is not closely related to *P. crucifer*; instead, *P. loligo*, which is characterized by a comparatively long branch, groups sister to *Actinostephanus* sp. (Actinodendridae), the latter of which is characterized by the longest branch in the phylogeny. BLAST results indicated that two of the three primer sets (18SA-L and 18SO-B) used to amplify 18S in *P. loligo* (see Rodríguez et al., 2012) may have amplified something other than *P. loligo*-specific 18S (details below). Thus, the relationship of *P. loligo* to *P. crucifer* is subject to change with the acquisition of new 18S sequence data for *P. loligo*.

We paired antipatharian-specific 28S primers with the standard sea anemone 28S primers to obtain 28S sequence data for 10 individuals from the GoM (representing all three morphotypes; see Table 6 for GenBank accession numbers) and a single individual from the MC (representing morphotype 1). As with 18S, all *Phymanthus* 28S sequences were added to the comprehensive dataset presented in Rodríguez et al. (2012) and a phylogeny was constructed using maximum likelihood (Figure 4). The 11 specimens of *P. crucifer* did not form a monophyletic clade. Similar to 18S, 8 of the 11 individuals (Clade 1) grouped sister to *Bundodactis verrucosa* and *Bunodosoma grandis* (Verrill, 1869) (both Actiniidae; bootstrap support was only 38%). The remaining three individuals (Clade 2) grouped distantly from conspecifics (i.e., they grouped sister to a clade comprised of Actiniidae, Preactinidae and Clade 1; bootstrap support: 54%). Six specimens, representing morphotypes 1 and 3, were identical to one another (all grouped in Clade 1); the remaining five specimens were of morphotypes 2 and 3 (grouping in Clade 1 and 2). Because we could not obtain 28S sequence data for *P. loligo*, it was not available for comparison.

3.3 | Characterization of *Phymanthus crucifer* PCR products using original 18S and 28S primers

In all but a single case, the original 18S and 28S primers preferentially amplified what was living inside and/or outside of *P. crucifer* or what *P. crucifer* had consumed. Nuclear 18S was amplified in three overlapping fragments. Primers 18SA-18SL yielded a 584 bp sequence that matched the following (based on a megablast search) at an e-value of ≤-100: Actiniaria (6 genera), Scleractinia (1), Porifera (4), Hemichordata (1) and viridiplantae (1). GenBank contains a large number of actiniarian 18S sequences, which suggests that the "actiniarian" sequences obtained in this search are not sea anemone sequences at all. One of the four genera included in these search results was *P. loligo*. Primers 18SO-18SB yielded a 216 bp

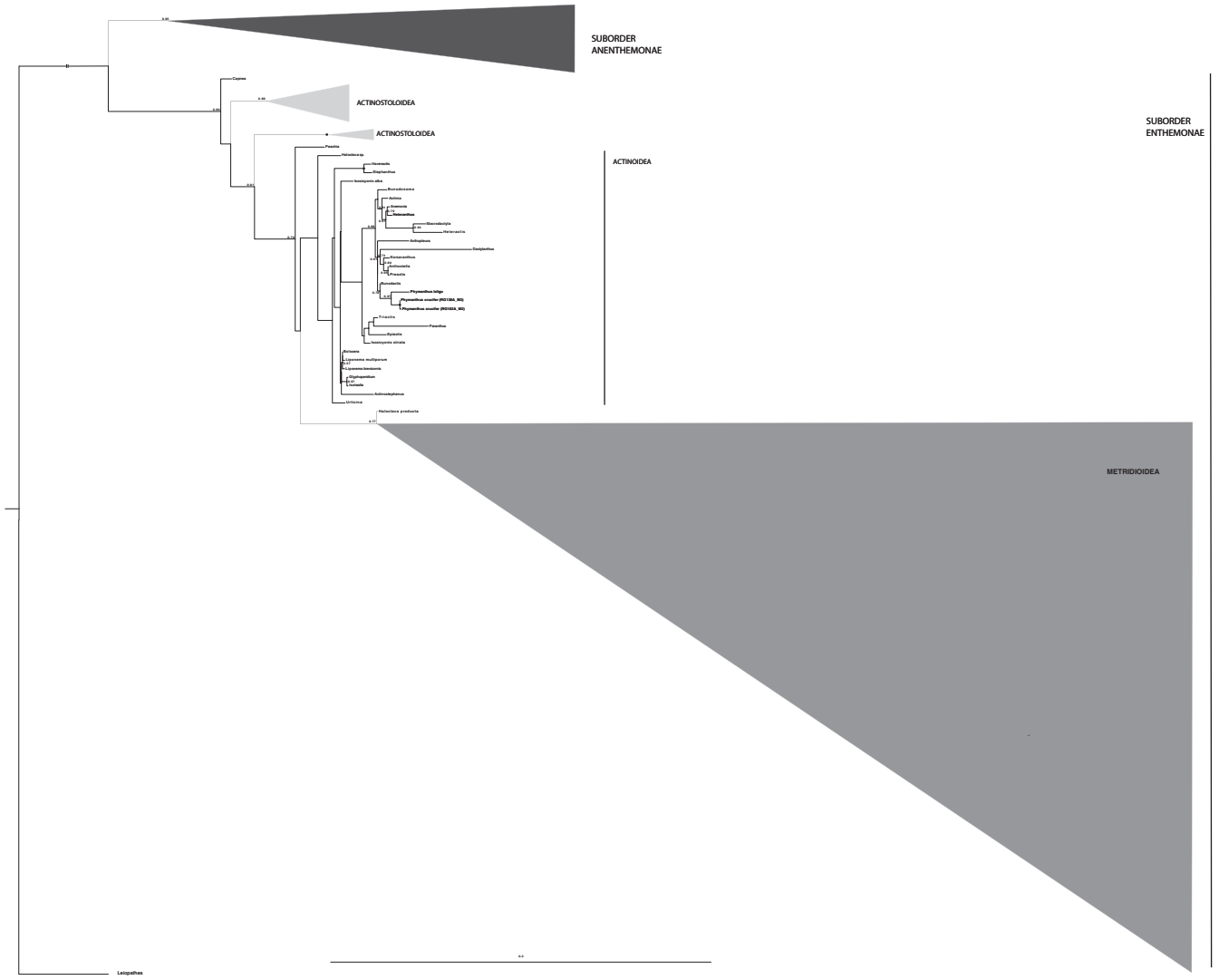

FIGURE 2 PhyML-based phylogenetic reconstruction of the Actiniaria using concatenated mitochondrial 12S, 16S and *cox3*. Individual specimens of the family Phymanthidae (*Phymanthus crucifer*, *P. loligo* and *Heteranthus* sp.) are in bold. Grey boxes indicate superfamilies within the order; the name of each superfamily is inside or next to the colored box; breath of boxes represents branch lengths. Species epithets are given only for genera represented by more than one species; for a complete list of taxa, see Rodríguez et al. (2012). Numbers above the branches are bootstrap resampling values; values <0.50 are not indicated; filled-in circles indicate nodes with support of 1.0. The phylogeny is rooted with the black coral *Leiopathes glaberrima*. M#: morphotype designation

sequence that had similar BLAST search results to 18SA-18SL (e-value ≤ −46): Actiniaria (3), Scleractinia (1), Hemichordata (2), Mollusca (1), Ceriantharia (1), Nemertea (1) and Echinodermata (2). Again, *P. loligo* was included in the list of actiniarians. Primers 18SC-18SY yielded a 682 bp sequence that returned the following best hits: for *P. crucifer* from the GoM: *Symbiodinium* sp. clade B (GenBank accession number KC848880); for *P. crucifer* from the MC: *Symbiodinium goreaui* Trench & Blank, 2000 strain CCMP 2466 (EF036539).

Nuclear 28S is typically amplified in five fragments, but only four primer sets yielded readable sequence data. Primers 5S-R635 yielded a 592 bp sequence for GoM *P. crucifer* (best hit: *Symbiodinium* sp. B1 [JN558057]) and a 593 bp sequence for MC *P. crucifer* (best hit: *Symbiodinium* sp. C90 [JN558047]). The latter BLAST search revealed that the publically available 28S sequence for *Heteractis aurora* (Quoy & Gaimard, 1833) (an actiniarian) actually belongs to *Symbiodinium* clade C. Primers F635-R1630 yielded a 796 bp sequence for GoM *P. crucifer* (best hit: the alveolate *Biecheleria brevisulcata* [AB858353]) and MC *P. crucifer* (best hit: *Symbiodinium* sp. Ulstrup [EF205017]). Primers F1379-R2077 yielded a 667 bp sequence for GoM *P. crucifer* (best hit: the alveolate *Gymnodiniaceae* sp. [FN552049]) and a 661 bp sequence for MC *P. crucifer* (best hit: FN552049). Primers F2076-R2800 yielded a 667 bp sequence for GoM *P. crucifer* (best hit: FN552049) and a 661 bp sequence for all but one MC *P. crucifer* (best hit: FN552049). Interestingly,

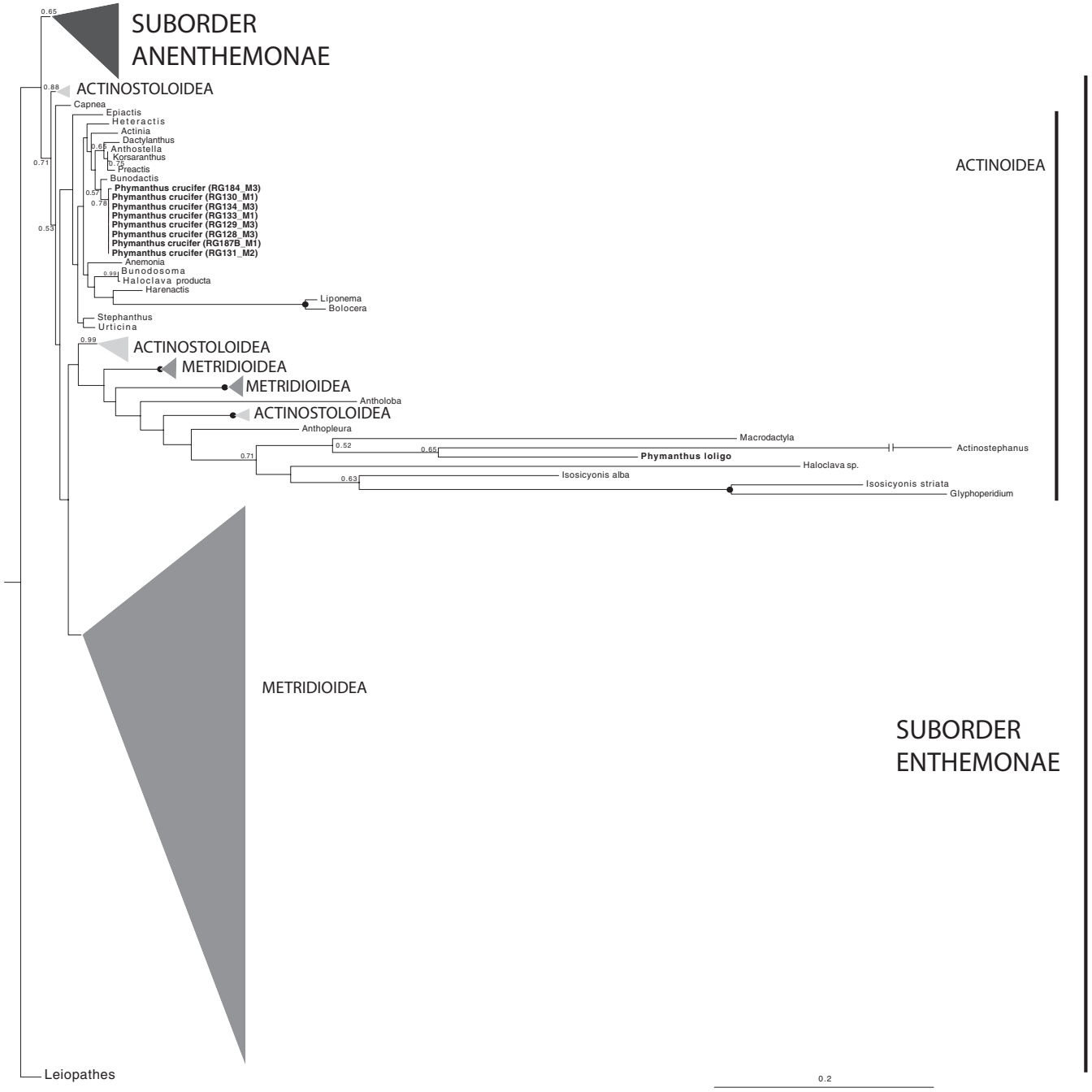

FIGURE 3 PhyML-based phylogenetic reconstruction of the Actiniaria using nuclear 18S rRNA. Individual specimens of the family Phymanthidae (*Phymanthus crucifer* and *P. loligo*) are in bold. The long branch leading to *Actinostephanus* has been shortened (indicated by a break) to increase readability. See Figure 2 legend for details on symbol usage and bootstrap support values

specimen RG-220A was characterized by a 731 bp sequence that was actually sea anemone specific. Based on the results above, it appears that *P. crucifer* from the GoM contains clade B *Symbiodinium* while individuals from the MC contain clade C *Symbiodinium*. Across all 18S and 28S primer sets, there was no variation within GoM or MC *P. crucifer*, but there was significant variation between individuals from the two localities.

3.4 | Characterization of the seven novel nuclear markers

The seven novel nuclear markers differed considerably in their length, ranging from 128 bp (Calpain [*i2*]) to 789 bp (Transferase [*i50*]) (amplicon lengths do not include primer sequences). Amplification of each of the seven novel nuclear markers resulted in a single, bright PCR product; however,

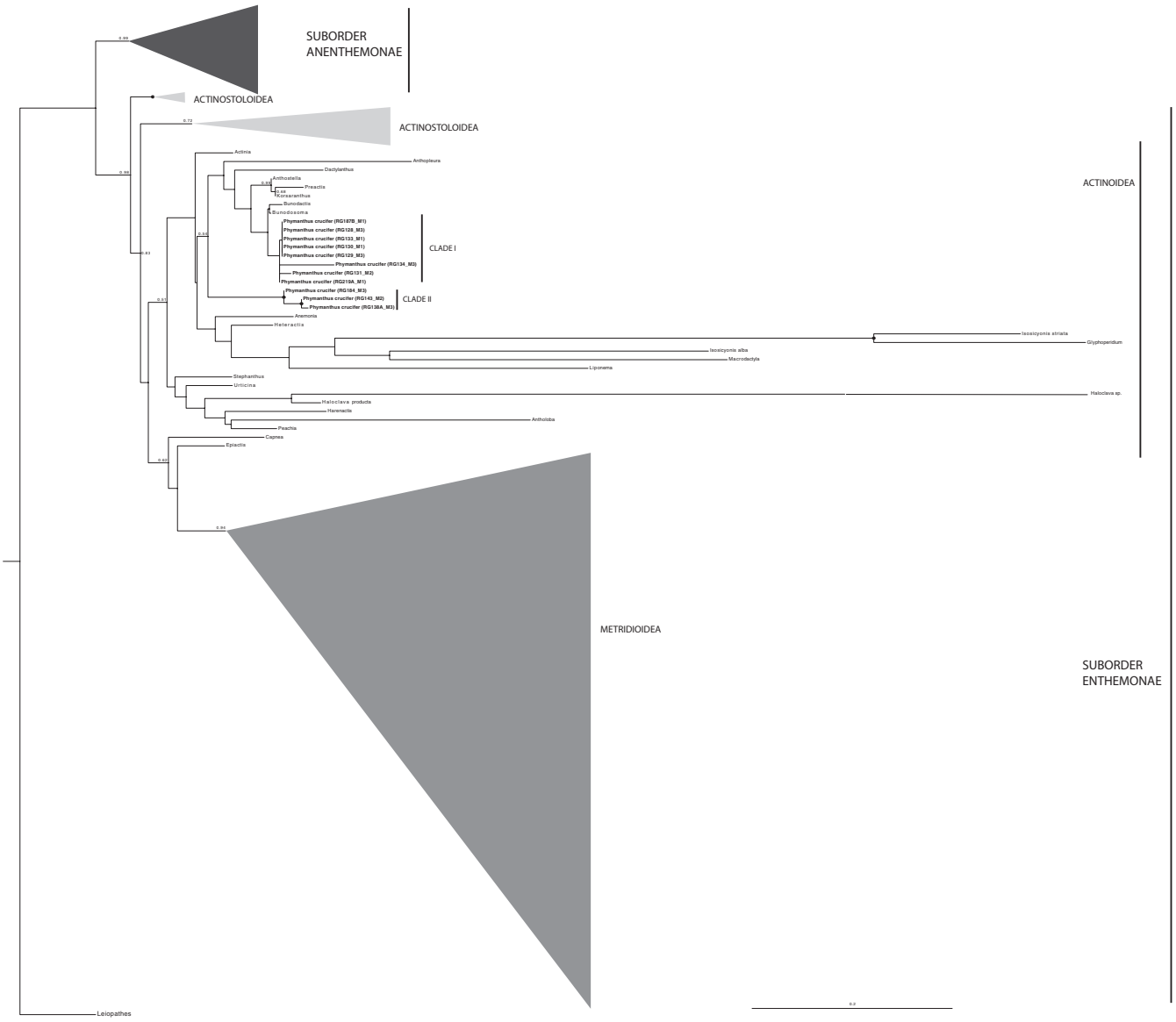

FIGURE 4 PhyML-based phylogenetic reconstruction of the Actiniaria using nuclear 28S rRNA. Individual specimens of *Phymanthus crucifer* are in bold. We were unable to obtain 28S sequence data for *P. loligo*. The long branch leading to *Haloclava* sp. has been shortened (indicated by a break) to increase readability. See Figure 2 legend for details on symbol usage and bootstrap support values

the raw chromatograms of all seven markers suggested the presence of two or more copies within a single individual (i.e., several positions along the chromatogram were characterized by double peaks). To determine the number of copies of each marker within a single individual, we cloned newly amplified PCR products of all seven genes. Specimens of *Phymanthus crucifer* from both the GoM and MC were selected for cloning; we also cloned the *CaM* intron in *P. loligo* to determine if any trends extended beyond *P. crucifer*. We screened upwards of 14 colonies per PCR product and, with the exception of Transferase (*i50*), recovered between 4 and 14 unique sequences per individual (Table 8). Cloning of PCR products for *Pes* (in specimen RG-187B) and *SRP54* (in specimen RG-219A) revealed a unique sequence in every bacterial colony that was screened (12 and 14, respectively; see Figure 5). Overall, intra-individual alleles were differentiated by not only nucleotide substitutions, but also length variation, as was the case for *CaM* (447/449 bp), *SRP54* (509/515 bp) and *VATPS-β* (584/585 bp). K2P distances among intra-individual alleles ranged from 1.39% for *SRP54* (in specimen RG-219A) to 13.79% for *Pes* (in specimen RG-187B) (Table 8; also see Table 6 for GenBank accession numbers).

We obtained DNA sequence data for Transferase (*i50*) from three individuals (RG-187B, RG-138A and RG-219A) and raw chromatograms from two of the three individuals (RG-187B and RG-219A) showed evidence of two or more alleles; however, only one of 12 screened clones (from specimen RG-219A) successfully incorporated PCR product. Therefore, we were unable to determine whether

TABLE 8 Cloning results and K2P distance estimates for six of the seven novel nuclear DNA markers in *Phymanthus crucifer*. The Calmodulin (*CaM*) intron was only cloned for *P. loligo* (specimen code PHY). *We originally obtained DNA sequence data for Transferase from three individuals (RG-187B, RG-138A, and RG-219A); however, only 1 of 12 screened clones successfully incorporated PCR product from specimen RG-219A

Nuclear marker	Specimen	Length (bp)	# Clones screened	# Unique sequences	# Variable sites	Range of K2P distances (%)
Calpain (*i2*)	RG-138A	128	11	5	8	0–5.72
Vacuolar ATP Synthase Subunit B (*VATPS-β*)	RG-187B	584, 585	12	9	15 + 1 bp indels ($n = 4$)	0–1.74
Signal Recog. Particle 54-kDa Subunit (*SRP54*)	RG-187B	509	12	9	13	0–1.59
Signal Recog. Particle 54-kDa Subunit (*SRP54*)	RG-219A	509, 515	14	14	18 + 6 bp indel	0–1.39
Pescadillo Homolog (*Pes*)	RG-187B	234	12	12	57	0.90–13.79
Nck Associated Protein 1 Homolog (*Nck*)	RG-219A	509	7	4	60	0–9.49
Transferase (*i50*)	RG-219A	789	12	N/A*	N/A	N/A
Calmodulin (*CaM*)	PHY	447, 449	11	9	17 + 2 bp indel	0–3.21

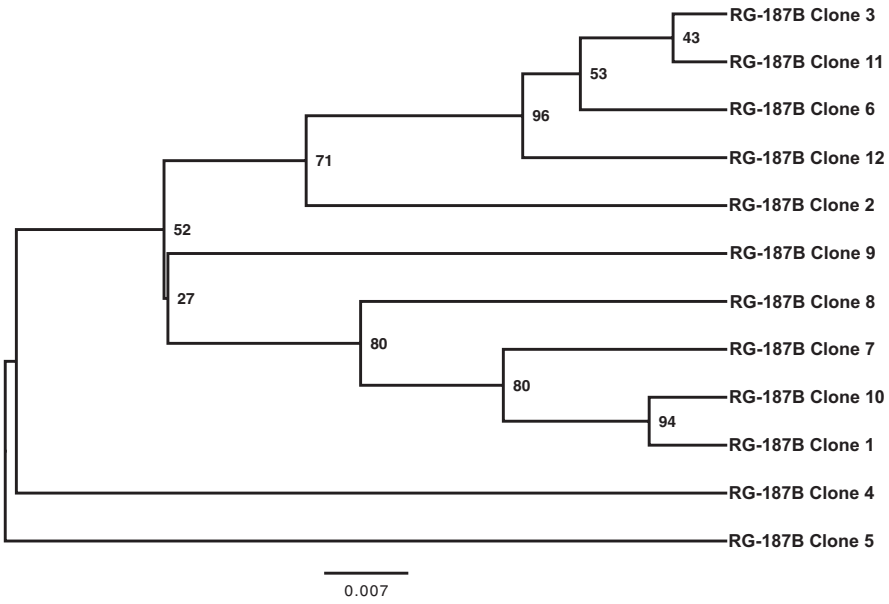

FIGURE 5 UPGMA tree of intra-individual alleles for the Pescadillo Homolog (*Pes*) within *Phymanthus crucifer* (specimen RG-187B). We screened 12 clones and recovered 12 different alleles with K2P distances ranging from 0.90% to 13.79%. Tree constructed with MEGA 5 using the following parameters: K2P model; substitutions included transitions and transversions; uniform rates among sites; pairwise deletion of gaps/missing data; 1,000 bootstrap replicates

specimen RG-219A is simply heterozygous for Transferase (*i50*) or whether Transferase (*i50*) is multi-copy. Similar to Transferase (*i50*), we obtained DNA sequence data for *CaM* from the same three individuals. Raw chromatograms from specimens RG-187B and RG-138A suggest that *P. crucifer* is heterozygous for *CaM* (RG-219A appeared homozygous); however, *CaM* was only cloned for *P. loligo*, not for *P. crucifer*. As shown in Table 8, 11 screened clones revealed 9 different *CaM* alleles within *P. loligo*, suggesting that the presence of two or more copies of a given marker within a single individual is not simply an isolated case within *P. crucifer* but rather more widespread.

Sequences from each of the seven novel nuclear markers were subjected to a BLAST search to determine if the targeted gene was successfully amplified. In the case of *CaM* and *VATPS-β*, the best hits were to an *Orthopyxis sargassicola* (Nutting, 1915) *CaM* gene (Hydrozoa; AY789838) and *Urticina eques* (Gosse, 1858) *VATPS-β* gene (Actiniaria; DQ988702), respectively; however, as a majority of each sequence was intronic, the above hits were based on a short section of exonic sequence. In the case of the other five nuclear markers (Calpain [*i2*], Transferase [*i50*], *Pes*, *Nck* and *SRP54*), no significant similarity was found when searching for highly similar sequences (megablast), more dissimilar sequences (discontinuous megablast) and somewhat similar sequences (blastn). These results are logical given that the nuclear markers were amplified using EPIC (exon-priming intron-crossing) primers; nearly all of the sequence data obtained for five of the seven nuclear markers is intronic.

4 | DISCUSSION

4.1 | Mitochondrial DNA

Mitochondrial *cox3* and 16S did not reveal any variation among individuals or morphotypes of *Phymanthus crucifer* from the GoM or MC. However, mitochondrial 12S did reveal two haplotypes. *Phymanthus loligo* shares an identical 12S sequence with *P. crucifer* H2 but has a K2P distance of 0.1233% when compared to *P. crucifer* H1. If *P. loligo* truly represents a distinct species and its K2P distance (when compared to *P. crucifer* H1) is indicative of that separate species status, then an argument can be made for the presence of two species among the *P. crucifer* specimens examined herein (i.e., 0.1215% vs. 0.1233%); however, current morphotype designations do not differentiate the two putative species of *P. crucifer*. Alternatively, if all three *P. crucifer* morphotypes are indeed a single species, then mitochondrial 12S revealed, for the first time, intraspecific variation within sea anemones.

4.2 | Nuclear rRNA

18S sequence data recovered the eight individuals of *Phymanthus crucifer* as single monophyletic clade. Seven specimens, representing all three morphotypes, were identical to one another, suggesting that marginal tentacle ornamentation occurs as a continuum from with to without ornamentation and is thus indicative of a single species. We also obtained 125 bp of 18S for specimen RG-143 (morphotype 2), which was identical to the seven specimens noted above (RG-143 was not included in the phylogeny). While 18S recovered a single clade of *P. crucifer*, 28S revealed the presence of two divergent clades. Clade 1 was comprised of eight specimens (including the only representative from the MC) while Clade 2 contained three specimens. These two clades do not appear to be separated based on geography (GoM vs. MC), morphotype (1, 2 or 3) or mitochondrial haplotype (H1 vs H2). The only individual from Clade 2 that is also represented in the 18S phylogeny is specimen RG-184 (morphotype 3), and RG-184 is the only individual in the 18S dataset with a unique sequence (differentiated by a single guanine substitution; K2P distance: 0.088%); but recall that this specimen displayed intra-individual variation at 18S when three partially overlapping PCR products were assembled (these were original amplicons, not cloned PCR products). We hypothesize that the sequences within Clade 2 are a result of 1) amplifying rRNA pseudogenes, 2) incomplete concerted evolution across rRNA repeats that is creating divergent paralogs or 3) incomplete lineage sorting among populations of *P. crucifer* that are potentially in the process of diverging, which is leading to a discordant phylogenetic reconstruction. However, given the large genetic distances between the two clades of *P. crucifer* (K2P between RG-133 and RG-138 is 11.67%; sequences for RG-134 and RG-138 do not overlap), an argument can be made for the presence of two different genera among our *P. crucifer* samples; however, this hypothesis is not supported morphologically and thus suggests that one of the three scenarios detailed above is leading to our spurious results. In the light of the presence of divergent 28S sequences within *P. crucifer*, we recommend that future studies increase taxon sampling at the intraspecific level (i.e., sequencing 28S in a single individual within Clade 1 or Clade 2 would lead to a very different set of inferred relationships). Six specimens, representing morphotypes 1 and 3, shared identical 28S sequences; the remaining five specimens were of morphotypes 2 and 3. Thus, 28S data suggest that having lateral protuberances in the marginal tentacles (morphotype 1) or being intermediate in form (morphotype 3) can occur within a single species, but specimens lacking protuberances (morphotype 2) may in the process of speciation and should be further scrutinized using more variable nuclear markers.

4.3 | Single or multi-copy markers?

Based on the results of cloned PCR products (i.e., there were more than two unique sequences per individual; Table 8), it would appear as though five of the seven novel nuclear markers are putatively multi-copy within *P. crucifer*. Although *CaM* was not cloned for *P. crucifer*, there was evidence of two or more copies based on the original raw chromatograms and cloning of *CaM* for *P. loligo* revealed nine different copies within a single individual. The same holds true for Transferase (*i50*); although 11 out of 12 screened clones did not yield readable sequence, there was evidence of two or more copies based on the original raw chromatograms. Multi-copy markers would suggest the presence of paralogs or polyploidy. However, taking into account *Taq* DNA polymerase error rates at both the PCR and cloning stage, the resulting variability is expected (i.e., the markers are not multi-copy). A review of the literature revealed a broad range of *Taq* error estimates: Cline, Braman, and Hogrefe (1996): 1.3×10^{-6} errors per site per duplication; Kobayashi, Tamura, and Aotsuka (1999): 7.3×10^{-5}; Thornhill, Lajeunesse, and Santos (2013): 1.21×10^{-4}. The error rate of the *Taq* Polymerase used in this study is estimated to be 2.2×10^{-5}. As an example, to calculate the expected number of errors per sequence for *SRP54*, we first estimated the number of errors per site by multiplying the *Taq* error rate (2.2×10^{-5}) by the total number of repeats (45 for PCR + 35 for cloning = 80), which is 1.76×10^{-3}. To estimate the number of errors per sequence, we multiplied the number of errors per site (1.76×10^{-3}) by the length of sequence (515 bp),

which yielded 0.9064 errors per sequence. Based on this calculation, we would expect approximately one error per sequence, and that is what we found for *SRP54*: we screened 14 clones, which revealed 14 unique sequences. The estimated number of errors per sequence for the other six nuclear markers is shown in Table 9. The only marker that yielded a significantly larger number of unique sequences than would be expected based on a *Taq* error rate of 2.2×10^{-5} is Pescadillo Homolog (*Pes*); the predicted number of errors per sequence for *Pes* (at 234 bp in length) is 0.41184, yet 12 out of 12 clones yielded unique sequences. Based on these results, it is our interpretation that at least six of the seven novel nuclear markers in *P. crucifer* do not have paralogs and these data do not suggest that the nuclear genome of *P. crucifer* is polyploid, but rather these are single copy markers in a diploid organism. A review of the literature reveals that ploidy within sea anemones ranges from $2n = 18$ (*Anthopleura midori* Uchida & Muramatsu, 1958 and *A. kurogane* Uchida & Muramatsu, 1958; Choe, Qi, & Song, 2000), 30 (*Nematostella vectensis*; Genikhovich & Technau, 2009) or 32 (*Diadumene lineata* (Verrill, 1869) [named as *Haliplanella luciae* (Verrill, 1898) in Fukui, 1993] and *Aiptasiomorpha* sp. [Fukui, 1996]). Additionally, the *Nematostella vectensis* nuclear genome (assembly ASM20922v1) shows no evidence of polyploidy.

4.4 | Application of novel markers within the three *Phymanthus crucifer* morphotypes

We successfully obtained sequence data from three of the seven novel nuclear markers (*i2* [150 bp], *Pes* [230 bp], *Nck* [557 bp]) for at least one representative of each morphotype (morphotype 1 contains lateral protuberances in the marginal tentacles; morphotype 2 lacks protuberances; morphotype 3 is intermediate in form; see Supporting Information Table S1). We were unable to obtain representative sequence data for morphotype 2 from *SRP54* [509 bp], *VATPS-β* [586 bp], *i50* [536 bp] and *CaM* [449 bp]. After visualizing the DNA extractions for specimens RG-182A and RG-220A (both morphotype 2) on a 1% agarose gel, we attribute this lack of amplification due to a lack of high molecular weight DNA. Based on the three markers that were sequenced for the three morphotypes (i.e., *i2*, *Pes* and *Nck*), there were no genetic differences observed among morphotypes. Sequence data for all seven markers was obtained for representatives of morphotypes 1 and 3, and, with the exception of a 2-bp indel in *CaM* for specimen RG-187B, no genetic differences were observed. These results suggest that the three morphotypes of *P. crucifer* represent a single species, despite differences in the presence or absence of protuberances in the marginal tentacles. We also successfully amplified and sequenced six of seven novel nuclear markers for *P. loligo* (we could not amplify *i50*). When compared to *P. crucifer*, there were no genetic differences observed at *SRP54* (495 bp comparable), *i2* (101 bp comparable), *Nck* (298 bp comparable) or *CaM* (420 bp comparable). However, there were two unique substitutions observed at *VATPS-β* (374 bp comparable) and 14 unique substitutions at *Pes* (113 bp comparable). These results suggest that *P. loligo* is a distinct species and that two of the seven new markers (i.e., *VATPS-β* and *Pes*) are better suited to elucidate interspecific variation within the Phymanthidae.

4.5 | Amplification of novel markers outside the Phymanthidae

To date, we have successfully amplified four of the seven novel nuclear markers (Calpain [*i2*], *VATPS-β*, Transferase [*i50*] and *CaM*)) within *Actinostola* (*A. chilensis* McMurrich, 1904, *A. crassicornis* (Hertwig, 1882) and *A. georgiana* Carlgren, 1927, as well as several undescribed species) (see Supporting Information Table S2). These results demonstrate the broad applicability of the new markers outside the Phymanthidae. We also obtained sequence data for three additional novel nuclear genes within *Actinostola* (Arginine Kinase [*AK*], Glyceraldehyde

TABLE 9 Estimated number of errors per sequence for the seven novel nuclear markers based on a *Taq* DNA Polymerase error rate of 2.2×10^{-5} errors per site per duplication and 80 repeats (45 for PCR+35 for cloning)

Nuclear marker	Length (bp)	Number of errors per sequence
Signal Recognition Particle 54-kDa Subunit (*SRP54*)	515	0.9064
Calpain (*i2*)	128	0.2253
Vacuolar ATP Synthase Subunit B (*VATPS-β*)	585	1.0296
Pescadillo Homolog (*Pes*)	234	0.4118
Nck Associated Protein 1 Homolog (*Nck*)	509	0.8958
Transferase (*i50*)	789	1.3886
Calmodulin (*CaM*)	449	0.7902

3-Phosphate Dehydrogenase [*G3PDH*] and 2-Phospho-D-Glycerate Hydrolase [*Enolase*]), all of which are putatively single copy based on cloning of PCR products (see Table 10 for primer sequences). Results of these new markers as applied to species within *Actinostola* will be discussed in a separate manuscript.

4.6 | A cautionary note regarding putative "single-copy" nuclear markers

Octocorallian and scleractinian systematists have a number of putatively single-copy nuclear markers at their disposal. For example, *SRP54* (Jarman et al., 2002) has been successfully used to elucidate cryptic species and address questions regarding phylogeography in the octocoral genus *Carijoa* Müller, 1867, as well as the scleractinian genus *Pocillopora* Lamarck, 1816 (Concepcion, Crepeau, Wagner, Kahng, & Toonen, 2008). Stemmer et al. (1997) utilized *SRP54* for species delimitations with the alcyonacean soft coral family Xeniidae Ehrenberg, 1828 while Watling and France (2001) used *SRP54* to characterize a new genus and species of deep-sea bamboo coral. *CaM* has been applied to questions concerning species delimitations (Chen et al., 2009) and the potential role of hybridization (Vollmer & Palumbi, 1995) in the scleractinian genus *Acropora* Oken, 1815. Hybridization in *Acropora* was also analysed using the minicollagen (*mcol*) gene (Hatta et al., 1999; Vollmer & Palumbi, 1995). Lastly, *Pax-C* (a *Pax-6* homolog) has been used to examine species boundaries among *Acropora cervicornis* (Lamarck, 1816), *A. palmata* (Lamarck, 1816) and *A. prolifera* (Lamarck, 1816) (van Oppen, Willis, Van Vugt, & Miller, 2000) and molecular relationships across a wide range of *Acropora* (van Oppen, McDonald, Willis, & Miller, 2001) and *Montipora* Blainville, 1830 (van Oppen, Koolmees, & Veron, 2004) species.

All of the above-mentioned studies explicitly state that the nuclear genes analysed are single copy. However, with the exception of Hatta et al. (1999), neither the author's analyses nor the papers they cite provide adequate support for such a statement. Concepcion et al. (2008) noted "a small number of samples (5 of 166) were found from which three alleles were identified during cloning, and all three alleles were clearly visible within the direct sequence for four of these five samples" and "in all cases clones were sequenced until multiple copies of each sequence were found." The authors failed to note how many clones were screened per individual and attributed the presence of multi-allelism to colony fusion. Stemmer et al. (1997) bypassed cloning completely and directly sequenced purified PCR products for *SRP54*. The authors noted that "at least" 7 of 75 individuals (9.3%) were found to have heterozygous genotypes and thus excluded them from their dataset. Watling and France (2001) also directly sequenced *SRP54* but noted extreme variability in intron length (92–934 bp) within and among Keratoisidinae genera (due to large indels); thus, *SRP54* was excluded from further consideration. Pante et al. (2012) presented a comprehensive phylogenetic analysis of the octocoral family Chrysogorgiidae Verrill, 1883 and discussed the need for informative markers that are variable at the intra- and inter-population level but noted that *SRP54* "is very challenging to work with in the Chrysogorgiidae" and accordingly did

TABLE 10 Primer sequence information for Arginine Kinase *(AK),* Glyceraldehyde 3-Phosphate Dehydrogenase (*G3PDH*) and 2-Phospho-D-Glycerate Hydrolase *(Enolase)*. ACT: actiniarian-specific primer. NV: *Nematostella vectensis*-specific primer

Gene	Primer name	T_M (°C)	Length (bp)	Number of ambiguities	Sequence (5′–3′)
Arginine Kinase (*AK*)[a]	AK-ACT-F	65.5	22	2	CAC ATC CAG GCS CGT GGM ATC C
	AK-ACT-R	60.7	27	1	GTT GAT GCA GTC GTA MAG GGA GAT TCC
Glyceraldehyde 3-Phosphate Dehydrogenase (*G3PDH*)[b]	G3P-ACT-F	60.1	22	1	GGT ATG GCA TTC CGT GTM CCT G
	G3P-ACT-R	63.2	24	4	CCC ATY TCT TTR GAC TCM GAK GCC
2-Phospho-D-Glycerate Hydrolase (*Enolase*)[c]	ENOL-NV-F2	56.8	20	2	ATT GGC ATG GAT GTW GCW GC
	ENOL-NV-R	60.7	31	0	CCC AAT GAT CTT GGT CAA AGG CAT CTT CAA T

[a]Original primers presented in Suzuki, Kawasaki, and Furukohri (2009). Used *Nematostella vectensis* and *Anthopleura japonicus* to develop new primers. Forward primer shifted slightly downstream from original Anth-F1 primer location; primer sits 148 bp from end of exon 5. Reverse primer shifted slightly downstream from original Anth-R3 primer location; primer sits 115 bp from beginning of exon 6.[b]The original primers presented in Bourlat et al. (2008) span an exon/intron boundary in *N. vectensis* so had to develop new primers in exon sequence only. Both primers developed using *Uticina eques* and *N. vectensis*. Forward primer is 48 bp away from end of exon 5. Reverse primer is 34 bp away from start of exon 6.[c]Original primers presented in Kelly and Palumbi (2009). Used *N. vectensis* to develop new primers.

not present any results. Chen et al. (2009) screened at least three clones per species for *CaM* and noted, "most species contain diverse alleles which cause the *CaM* intron phylogeny to be not monophyletic." Because information is not provided as to how many individuals per species were analysed, it is difficult to interpret the *CaM* intron phylogeny presented in Figure 3 of Chen et al. (2009). For example, there are five *Acropora aculeus* (Dana, 1846) (specimen ID# NQ381) sequences spread throughout the *CaM* phylogeny, four of five of which are extremely divergent from one another (corresponding GenBank records suggest that each sequence represents a distinct clone from a single individual). Additionally, the seminal paper that was cited as showing that the *A. muricata* (Linnaeus, 1758) *CaM* gene is single copy (Chiou et al., 2008) is technically flawed. Genomic DNA was extracted from sperm, which contains only a single copy of the genome, and transferred onto a membrane for use in a Southern blot analysis (probed with a 395 bp coral *CaM* genomic DNA and 232 bp coral *CaM* cDNA fragment); however, if multiple copies of the *CaM* gene are embedded within the egg genome but not the sperm genome, its multi-copy nature would not be detected using sperm DNA only. Vollmer and Palumbi (1995) noted that amplifications of *CaM* were sequenced directly and heterozygous nuclear alleles were simply observed as double peaks, which leaves open the possibility that more than two alleles were present if two or more occurrences of double peaks were detected at discrete positions along the sequence (number of double peaks not addressed). van Oppen et al. (2000) directly sequenced the *Pax-C* intron from PCR products because "levels of variability were low and no variability in length was observed," although the authors do not discuss what is meant by low levels of variability. Sequence ambiguities were interpreted as heterozygosity; however, the authors provide six examples for which ambiguities were found at more than one position, four of which had at least three different alleles. The authors note that the single-copy nature of *Pax-C* is confirmed in a study—published a year later—by van Oppen et al. (2001); however, in the 2001 paper, the authors cite Callaerts, Halder, and Gehring (1997) as confirming the single-copy nature of *Pax-C*; a review of Callaerts et al. (1997) returns no mention of *Pax-C* being single copy. van Oppen et al. (2001) initially screened 2–7 clones for a subset of coral colonies, and subsequently screened a maximum of four clones per colony to determine whether the colony was heterozygous for *Pax-C*. The authors noted that there were a "few instances in which more than two sequences per individuals were found, (but) these differed by only one or two point mutations which were not shared by other clones, suggesting that these were PCR errors and that no more than two alleles were present per diploid genome," but later noted "alleles within individuals showed considerable sequence divergence in many cases." van Oppen et al. (2004) screened 1–3 clones per individual and found at least four cases in which three different alleles were revealed (*Montipora* sp. 1, *M. confusa* Nemenzo, 1967, *M. aequituberculata* Bernard, 1897, *M. spongodes* Bernard, 1897); instead of acknowledging or discussing these results, the authors again cite Callaerts et al. (1997) as confirming the single-copy nature of *Pax-C* (the authors also cite Catmull et al., 1998; but as with Callaerts et al., 1997, no mention is made to *Pax-C* being single copy).

Hatta et al. (1999) appears to be the only study that provided rigorous support for their gene of interest (minicollagen) being single copy; the authors screened at least five clones per individual (from one to three independent PCRs) and cited a study that explicitly isolated and characterized *mcol* as single copy in *Acropora donei* Veron & Wallace, 1984 (Wang et al., 2011). Thus, it is our recommendation that scleractinian systematists consider using *mcol* in future molecular-based studies as opposed to *SRP54*, *CaM* or *Pax-C* as evidence suggests that these latter three genes may be multi-copy. An alternative explanation is that the *Taq* DNA Polymerase utilized in some of the above mentioned studies may not have been high fidelity and thus *Taq* errors during PCR and/or cloning can account for the observed variation.

5 | CONCLUSIONS

Herein, we evaluated whether morphological variability in marginal tentacle protuberances is indicative of intraspecific variation or cryptic species in the shallow-water sea anemone *Phymanthus crucifer*. External and internal morphological features, cnidae, mitochondrial DNA, 18S rDNA, as well as the novel nuclear markers presented herein all suggest that the three morphotypes of *P. crucifer* represent a single species, despite differences in the presence or absence of protuberances in the marginal tentacles. Our data support Duerden (1897, 1900, 1902), who noted that the presence of intermediate forms suggests a continuum from with to without marginal tentacle protuberances (ornamentation) and thus is indicative of a single species. The significance and function of the protuberances in the marginal tentacles remains unknown within *P. crucifer* but might be related to specific adaptations to the surrounding environment. Since all three *P. crucifer* morphotypes are indeed a single species, then mitochondrial 12S revealed, for the first time, intraspecific variation within sea anemones. Future studies analysing intraspecific variation within the Actiniaria should consider testing all seven novel nuclear markers presented herein; however, we suggest starting with Calpain (*i2*) and Nck-Associated Protein 1 Homolog (*Nck*) and recommend cloning the PCR

products of Pescadillo Homolog (*Pes*) as our data suggest the presence of multiple copies in *P. crucifer*. For interspecific comparisons, we recommend *Pes* and Vacuolar ATP Synthase Subunit B (*VATPS*-β), and for intergeneric comparisons, we recommend *i2*, *VATPS-β*, Transferase (*i50*) and Calmodulin (*CaM*). Lastly, regardless of the taxonomic rank being compared, we recommend amplifying *i2* within older (museum) material as the amplicon is only ~128 bp in length.

ACKNOWLEDGEMENTS

MRB was initially supported by a postdoctoral fellowship from coauthor ER. MRB also received generous postdoctoral funding from the Gerstner Family Foundation and the AMNH's Richard Gilder Graduate School. All specimens were collected under consent of Mexican law; the collecting permit was approved by Comisión Nacional de Acuacultura y Pesca (#07332.250810.4060). We thank Drs. Nuno Simões (UMDI-Sisal-UNAM) and Judith Sánchez (ICMyL-UNAM) as well as the Comisión Nacional de Áreas Naturales Protegidas (CONANP) for their assistance with fieldwork.

ORCID

Mercer R. Brugler http://orcid.org/0000-0003-3676-1226

REFERENCES

Altschul, S. F., Gish, W., Miller, W., Myers, E. W., & Lipman, D. J. (1990). Basic local alignment search tool. *Journal of Molecular Biology*, *215*(3), 403–410.

Bourlat, S. J., Nielsen, C., Economou, A. D., & Telford, M. J. (2008). Testing the new animal phylogeny: A phylum level molecular analysis of the animal kingdom. *Molecular Phylogenetics and Evolution*, *49*(1), 23–31.

Brugler, M. R., Opresko, D. M., & France, S. C. (2013). The evolutionary history of the order Antipatharia (Cnidaria: Anthozoa: Hexacorallia) as inferred from mitochondrial and nuclear DNA: Implications for black coral taxonomy and systematics. *Zoological Journal of the Linnean Society*, *169*(2), 312–361.

Callaerts, P., Halder, G., & Gehring, W. J. (1997). PAX-6 in development and evolution. *Annual Review of Neuroscience*, *20*(1), 483–532.

Cappola, V. A., & Fautin, D. G. (2000). All three species of Ptychodactiaria belong to order Actiniaria (Cnidaria: Anthozoa). *Journal of the Marine Biological Association of the United Kingdom*, *80*(6), 995–1005.

Carlgren, O. H. (1949). *A survey of the Ptychodactiaria, Corallimorpharia and Actiniaria* (Vol. *1*). Uppsala, Sweden: Almqvist & Wiksells boktr.

Catmull, J., Hayward, D. C., McIntyre, N. E., Reece-Hoyes, J. S., Mastro, R., Callaerts, P., … Miller, D. J. (1998). Pax-6 origins–implications from the structure of two coral Pax genes. *Development Genes and Evolution*, *208*(6), 352–356.

Chen, C., Chiou, C. Y., Dai, C. F., & Chen, C. A. (2008). Unique mitogenomic features in the scleractinian family Pocilloporidae (Scleractinia: Astrocoeniina). *Marine Biotechnology*, *10*(5), 538–553.

Chen, C., Dai, C. F., Plathong, S., Chiou, C. Y., & Chen, C. A. (2008). The complete mitochondrial genomes of needle corals, *Seriatopora* spp. (Scleractinia: Pocilloporidae): An idiosyncratic atp8, duplicated trnW gene, and hypervariable regions used to determine species phylogenies and recently diverged populations. *Molecular Phylogenetics and Evolution*, *46*(1), 19–33.

Chen, I. P., Tang, C. Y., Chiou, C. Y., Hsu, J. H., Wei, N. V., Wallace, C. C., … Chen, C. A. (2009). Comparative analyses of coding and noncoding DNA regions indicate that *Acropora* (Anthozoa: Scleractina) possesses a similar evolutionary tempo of nuclear vs. mitochondrial genomes as in plants. *Marine Biotechnology*, *11*(1), 141–152.

Chenuil, A., Hoareau, T. B., Egea, E., Penant, G., Rocher, C., Aurelle, D., … Krakau, M. (2010). An efficient method to find potentially universal population genetic markers, applied to metazoans. *BMC Evolutionary Biology*, *10*(1), 276.

Chiou, C. Y., Chen, I. P., Chen, C., Wu, H. J. L., Wei, N. V., Wallace, C. C., & Chen, C. A. (2008). Analysis of *Acropora muricata* calmodulin (CaM) indicates that scleractinian corals possess the ancestral Exon/Intron organization of the eumetazoan CaM gene. *Journal of Molecular Evolution*, *66*(4), 317–324.

Choe, B. L., Qi, H., & Song, J. I. (2000). Karyotypes of two sea anemones (Cnidaria; Anthozoa) from Korea. *Korean Journal of Biological Sciences*, *4*(2), 103–104.

Cline, J., Braman, J. C., & Hogrefe, H. H. (1996). PCR fidelity of Pfu DNA polymerase and other thermostable DNA polymerases. *Nucleic Acids Research*, *24*(18), 3546–3551.

Concepcion, G. T., Crepeau, M. W., Wagner, D., Kahng, S. E., & Toonen, R. J. (2008). An alternative to ITS, a hypervariable, single-copy nuclear intron in corals, and its use in detecting cryptic species within the octocoral genus *Carijoa*. *Coral Reefs*, *27*(2), 323–336.

Daly, M. (2006). Boloceroides daphneae, a new species of giant sea anemone (Cnidaria: Actiniaria: Boloceroididae) from the deep Pacific. *Marine Biology*, *148*(6), 1241–1247.

Daly, M., Chaudhuri, A., Gusmão, L., & Rodriguez, E. (2008). Phylogenetic relationships among sea anemones (Cnidaria: Anthozoa: Actiniaria). *Molecular Phylogenetics and Evolution*, *48*(1), 292–301.

Daly, M., & Fautin, D. (2018). World List of Actiniaria. *Phymanthus* Milne Edwards & Haime, 1851. Retrieved World Register of Marine Species from http://www.marinespecies.org/aphia.php?p=taxdetails&xml:id=100772 (Accessed on 2018-04-29)

Daly, M., Fautin, D. G., & Cappola, V. A. (2003). Systematics of the Hexacorallia (Cnidaria: Anthozoa). *Zoological Journal of the Linnean Society*, *139*(3), 419–437.

Daly, M., Gusmão, L. C., Reft, A. J., & Rodríguez, E. (2010). Phylogenetic signal in mitochondrial and nuclear markers in sea anemones (Cnidaria, Actiniaria). *Integrative and Comparative Biology*, *50*(3), 371–388.

Darriba, D., Taboada, G. L., Doallo, R., & Posada, D. (2012). jModelTest 2: More models, new heuristics and parallel computing. *Nature Methods*, *9*(8), 772.

Duerden, J. E. (1897). I.—The Actiniarian family Aliciidæ. *Journal of Natural History*, *20*(115), 1–15.

Duerden, J. E. (1900). Jamaican Actiniaria. Part II. Stichodactylinæ and *Zoantheae*. *Scientific Transactions of the Royal Dublin Society*, *7*, 133–208.

Duerden, J. E. (1902). Report of the Actinians of Porto Rico (Investigations of the aquatic resources and fisheries of Porto Rico by the U.S. Fish Commission Steamer Fish Hawk in 1899). *Bulletin of the U.S. Fish Commission*, *20*, 323–374.

Ehrenberg, C. G. (1834). Beiträge zur physiologischen Kenntniss der Corallenthiere im allgemeinen, und besonders des rothen Meeres, nebst einem Versuche zur physiologischen Systematik derselben. *Abhandlungen der Königlichen Akademie der Wissenschaften zu Berlin*, *1*, 225–380.

Forsman, Z. H., Barshis, D. J., Hunter, C. L., & Toonen, R. J. (2009). Shape-shifting corals: Molecular markers show morphology is evolutionarily plastic in Porites. *BMC Evolutionary Biology*, *9*(1), 45.

Fukui, Y. (1993). Chromosomes of the sea anemone *Haliplanella luciae* (= *H. lineata*)(Coelenterata: Actiniaria). *Journal of the Marine Biological Association of the United Kingdom*, *73*(4), 971–973.

Fukui, Y. (1996). Karyotype of the sea anemone *Aiptasiomorpha* sp. (Anthozoa, Actiniaria) from Japan. *The Biological Bulletin*, *190*(1), 6–7.

Geller, J. B., Fitzgerald, L. J., & King, C. E. (2005). Fission in sea anemones: Integrative studies of life cycle evolution. *Integrative and Comparative Biology*, *45*(4), 615–622.

Genikhovich, G., & Technau, U. (2009). The starlet sea anemone *Nematostella vectensis*: An anthozoan model organism for studies in comparative genomics and functional evolutionary developmental biology. *Cold Spring Harbor Protocols*, *2009*(9), pdb.emo129.

González-Muñoz, R., Simões, N., Mascaró, M., Tello-Musi, J. L., Brugler, M. R., & Rodríguez, E. (2015). Morphological and molecular variability of the sea anemone *Phymanthus crucifer* (Cnidaria, Anthozoa, Actiniaria, Actinoidea). *Journal of the Marine Biological Association of the United Kingdom*, *95*(1), 69–79.

Gonzalez-Munoz, R., Simoes, N., Sanchez-Rodriguez, J., Rodriguez, E., & Segura-Puertas, L. (2012). First inventory of sea anemones (Cnidaria: Actiniaria) of the Mexican Caribbean. *Zootaxa*, *3556*, 1–38.

Grajales, A., & Rodríguez, E. (2016). Elucidating the evolutionary relationships of the Aiptasiidae, a widespread cnidarian–dinoflagellate model system (Cnidaria: Anthozoa: Actiniaria: Metridioidea). *Molecular Phylogenetics and Evolution*, *94*, 252–263.

Guindon, S., Dufayard, J. F., Lefort, V., Anisimova, M., Hordijk, W., & Gascuel, O. (2010). New algorithms and methods to estimate maximum-likelihood phylogenies: Assessing the performance of PhyML 3.0. *Systematic Biology*, *59*(3), 307–321.

Guindon, S., & Gascuel, O. (2003). A simple, fast, and accurate algorithm to estimate large phylogenies by maximum likelihood. *Systematic Biology*, *52*(5), 696–704.

Gusmão, L. C., & Daly, M. (2010). Evolution of sea anemones (Cnidaria: Actiniaria: Hormathiidae) symbiotic with hermit crabs. *Molecular Phylogenetics and Evolution*, *56*(3), 868–877.

Hatta, M., Fukami, H., Wang, W., Omori, M., Shimoike, K., Hayashibara, T., … Sugiyama, T. (1999). Reproductive and genetic evidence for a reticulate evolutionary history of mass-spawning corals. *Molecular Biology and Evolution*, *16*(11), 1607–1613.

Hellberg, M. E. (2006). No variation and low synonymous substitution rates in coral mtDNA despite high nuclear variation. *BMC Evolutionary Biology*, *6*(1), 24.

Jarman, S. N., Ward, R. D., & Elliott, N. G. (2002). Oligonucleotide primers for PCR amplification of coelomate introns. *Marine Biotechnology*, *4*(4), 347–355.

Katoh, K., Kuma, K. I., Toh, H., & Miyata, T. (2005). MAFFT version 5: Improvement in accuracy of multiple sequence alignment. *Nucleic Acids Research*, *33*(2), 511–518.

Katoh, K., Misawa, K., Kuma, K. I., & Miyata, T. (2002). MAFFT: A novel method for rapid multiple sequence alignment based on fast Fourier transform. *Nucleic Acids Research*, *30*(14), 3059–3066.

Kelly, R. P., & Palumbi, S. R. (2009). General-use polymerase chain reaction primers for amplification and direct sequencing of enolase, a single-copy nuclear gene, from different animal phyla. *Molecular Ecology Resources*, *9*(1), 144–147.

Kobayashi, N., Tamura, K., & Aotsuka, T. (1999). PCR error and molecular population genetics. *Biochemical Genetics*, *37*(9), 317–321.

Lauretta, D., Häussermann, V., Brugler, M. R., & Rodríguez, E. (2014). *Isoparactis fionae* sp. nov. (Cnidaria: Anthozoa: Actiniaria) from Southern Patagonia with a discussion of the family Isanthidae. *Organisms Diversity & Evolution*, *14*(1), 31–42.

Le Sueur, C. A. (1817). Observations on several species of genus actinia; illustrated by figures: read Dec. 9, 1817. *Journal of the Academy of Natural Sciences of Philadelphia*, *1*, 149–154, 169–189.

Mallien, C., Porro, B., Zamoum, T., Olivier, C., Wiedenmann, J., Furla, P., & Forcioli, D. (2018). Conspicuous morphological differentiation without speciation in *Anemonia viridis* (Cnidaria, Actiniaria). *Systematics and Biodiversity*, *16*(3), 271–286.

McFadden, C. S., Benayahu, Y., Pante, E., Thoma, J. N., Nevarez, P. A., & France, S. C. (2011). Limitations of mitochondrial gene barcoding in Octocorallia. *Molecular Ecology Resources*, *11*(1), 19–31.

Milne-Edwards, H., & Haime, J. (1851). *Archives du Muséum d'Historie Naturelle. 5: Monographie des polypiers fossils des terrains palfozooques, pricidie d'un tableau general de la classification des polypes* (p. 502). Paris, France: Gide et J. Baudry.

van Oppen, M. J. H., Koolmees, E. M., & Veron, J. E. N. (2004). Patterns of evolution in the scleractinian coral genus *Montipora* (Acroporidae). *Marine Biology*, *144*(1), 9–18.

van Oppen, M. J., McDonald, B. J., Willis, B., & Miller, D. J. (2001). The evolutionary history of the coral genus Acropora (Scleractinia, Cnidaria) based on a mitochondrial and a nuclear marker: Reticulation, incomplete lineage sorting, or morphological convergence? *Molecular Biology and Evolution*, *18*(7), 1315–1329.

van Oppen, M. J. H., Willis, B. L., Van Vugt, H. W. J. A., & Miller, D. J. (2000). Examination of species boundaries in the *Acropora cervicornis* group (Scleractinia, Cnidaria) using nuclear DNA sequence analyses. *Molecular Ecology*, *9*(9), 1363–1373.

Pante, E., France, S. C., Couloux, A., Cruaud, C., McFadden, C. S., Samadi, S., & Watling, L. (2012). Deep-sea origin and in-situ diversification of chrysogorgiid octocorals. *PLoS ONE*, *7*(6), e38357.

Rodríguez, E., Barbeitos, M. S., Brugler, M. R., Crowley, L. M., Grajales, A., Gusmão, L., … Daly, M. (2014). Hidden among sea anemones: The first comprehensive phylogenetic reconstruction of the order Actiniaria (Cnidaria, Anthozoa, Hexacorallia) reveals a novel group of hexacorals. *PLoS ONE*, *9*(5), e96998.

Rodríguez, E., Barbeitos, M., Daly, M., Gusmao, L. C., & Häussermann, V. (2012). Toward a natural classification: Phylogeny of acontiate sea anemones (Cnidaria, Anthozoa, Actiniaria). *Cladistics*, *28*(4), 375–392.

Rodríguez, E., & Daly, M. (2010). Phylogenetic relationships among deep-sea and chemosynthetic sea anemones: Actinoscyphiidae and Actinostolidae (Actiniaria: Mesomyaria). *PLoS ONE*, *5*(6), e10958.

Shearer, T. L., & Coffroth, M. A. (2008). DNA BARCODING: Barcoding corals: Limited by interspecific divergence, not intraspecific variation. *Molecular Ecology Resources*, *8*(2), 247–255.

Shearer, T. L., Van Oppen, M. J. H., Romano, S. L., & Wörheide, G. (2002). Slow mitochondrial DNA sequence evolution in the Anthozoa (Cnidaria). *Molecular Ecology*, *11*(12), 2475–2487.

Stampar, S. N., Maronna, M. M., Kitahara, M. V., Reimer, J. D., & Morandini, A. C. (2014). Fast-evolving mitochondrial DNA in Ceriantharia: A reflection of Hexacorallia paraphyly? *PLoS ONE*, *9*(1), e86612.

Stemmer, K., Burghardt, I., Mayer, C., Reinicke, G. B., Wägele, H., Tollrian, R., & Leese, F. (2013). Morphological and genetic analyses of xeniid soft coral diversity (Octocorallia; Alcyonacea). *Organisms Diversity & Evolution*, *13*(2), 135–150.

Suzuki, T., Kawasaki, Y., & Furukohri, T. (1997). Evolution of phosphagen kinase1: Isolation, characterization and cDNA-derived amino acid sequence of two-domain arginine kinase from the sea anemone *Anthopleura japonicus*. *Biochemical Journal*, *328*(1), 301–306.

Thoma, J. N., Pante, E., Brugler, M. R., & France, S. C. (2009). Deep-sea octocorals and antipatharians show no evidence of seamount-scale endemism in the NW Atlantic. *Marine Ecology Progress Series*, *397*, 25–35.

Thornhill, D. J., Lajeunesse, T. C., & Santos, S. R. (2007). Measuring rDNA diversity in eukaryotic microbial systems: How intragenomic variation, pseudogenes, and PCR artifacts confound biodiversity estimates. *Molecular Ecology*, *16*(24), 5326–5340.

UniProt Consortium (2013). Update on activities at the Universal Protein Resource (UniProt) in 2013. *Nucleic Acids Research*, *41*, D43–D47.

Verrill, A. E. (1900). Additions to the Anthozoa and Hydrozoa of the Bermudas. *Transaction of the Connecticut Academy of Arts and Sciences*, *10*, 551–572.

Verrill, A. E. (1907). The Bermuda Islands. Part IV. Geology and paleontology, and Part V. An account of the coral reefs. *Transactions of Connecticut Academic of Arts and Sciences*, *12*, 45–348.

Vollmer, S. V., & Palumbi, S. R. (2002). Hybridization and the evolution of reef coral diversity. *Science*, *296*(5575), 2023–2025.

Wang, W., Omori, M., Hayashibara, T., Shimoike, K., Hatta, M., Sugiyama, T., & Fujisawa, T. (1995). Isolation and characterization of a mini-collagen gene encoding a nematocyst capsule protein from a reef-building coral, *Acropora donei*. *Gene*, *152*(2), 195–200.

Watling, L., & France, S. C. (2011). A new genus and species of bamboo coral (Octocorallia: Isididae: Keratoisidinae) from the New England seamounts. *Bulletin of the Peabody Museum of Natural History*, *51*(2), 209–220.

Yuasa, H. J., Suzuki, T., & Yazawa, M. (2001). Structural organization of lower marine nonvertebrate calmodulin genes. *Gene*, *279*(2), 205–212.

SUPPORTING INFORMATION

Additional supporting information may be found online in the Supporting Information section at the end of the article.

How to cite this article: Brugler MR, González-Muñoz RE, Tessler M, Rodríguez E. An EPIC journey to locate single-copy nuclear markers in sea anemones. *Zool Scr*. 2018;47:756–776. https://doi.org/10.1111/zsc.12309